HHS Public Access

Author manuscript

Nat Med. Author manuscript; available in PMC 2020 September 02.

Published in final edited form as:

Nat Med. 2020 March ; 26(3): 387–397. doi:10.1038/s41591-020-0762-2.

Diagnostic value of plasma phosphorylated tau181 in Alzheimer's disease and frontotemporal lobar degeneration

Elisabeth H. Thijssen, MS[1,2], Renaud La Joie, PhD[1], Amy Wolf, BS[1], Amelia Strom, BS[1], Ping Wang, MS[1], Leonardo Iaccarino, PhD[1], Viktoriya Bourakova, BA[1], Yann Cobigo, PhD[1], Hilary Heuer, PhD[1], Salvatore Spina, MD, PhD[1], Lawren VandeVrede, MD, PhD[1], Xiyun Chai, MD[3], Nicholas K. Proctor, BS[3], David C. Airey, PhD[3], Sergey Shcherbinin, PhD[3], Cynthia Duggan Evans, PhD[3], John R. Sims, MD[3], Henrik Zetterberg, MD, PhD[4,5,6,7], Kaj Blennow, MD, PhD[4,5], Anna M. Karydas, BA[1], Charlotte E. Teunissen, PhD[2], Joel H. Kramer, PsyD[1], Lea T. Grinberg, MD, PhD[1,8], William W. Seeley, MD[1,8], Howie Rosen, MD[1], Bradley F. Boeve, MD[9], Bruce L. Miller, MD[1], Gil D. Rabinovici, MD[1,10], Jeffrey L. Dage, PhD[3], Julio C. Rojas, MD, PhD[1], Adam L. Boxer, MD, PhD[1,a] Advancing Research and Treatment for Frontotemporal Lobar Degeneration (ARTFL) investigators

[1.]Memory and Aging Center, Department of Neurology, University of California, San Francisco, California, United States of America [2.]Neurochemistry Laboratory, Department of Clinical Chemistry, Amsterdam University Medical Centers, Vrije Universiteit, Amsterdam Neuroscience,

[a]To whom correspondence should be addressed: 675 Nelson Rising Lane, Suite 190, MC 1207, San Francisco, CA, 94158, adam.boxer@ucsf.edu.

Author contributions:

E.H.T. and J.C.R. had full access to all of the data in the study and take responsibility for the integrity of the data and the accuracy of the data analysis.

Concept and design: E.H.T., J.L.D, J.C.R., A.L.B.

Acquisition, analysis, or interpretation of data: All authors.

Drafting of the manuscript: E.H.T.

Critical revision of the manuscript for important intellectual content: E.H.T., R.L.J., J.L.D., J.C.R., A.L.B.

Statistical analysis: E.H.T., R.L.J., P.W., D.C.A., J.C.R.

Obtained funding: A.L.B., B.F.B., H.R., B.L.M., G.D.R., J.H.K., J.L.D.

Supervision: J.L.D., J.C.R., A.L.B.

Competing interest statement:

E.H.T, R.L.J., A.W., A.S., P.W., L.I., V.B., Y.C., H.H., S.S., A.M.K., C.E.T., J.H.K., W.W.S., H.R., B.F.B., and B.L.M. declare no conflict of interest. J.L.D., X.C., N.K.P., D.C.A., S.S., C.D.E., and J.R.S. are employees of Eli Lilly and Company. H.Z. has served at scientific advisory boards for Roche Diagnostics, Wave, Samumed and CogRx, has given lectures in symposia sponsored by Alzecure and Biogen, and is a co-founder of Brain Biomarker Solutions in Gothenburg AB, a GU Ventures-based platform company at the University of Gothenburg. K.B. served as a consultant or at advisory boards for Alector, Biogen, CogRx, Lilly, MagQu, Novartis and Roche Diagnostics, and is a co-founder of Brain Biomarker Solutions in Gothenburg AB, a GU Venture-based platform company at the University of Gothenburg, all unrelated to the work presented in this paper. L.T.G. receives research support from Avid Radiopharmaceuticals, Eli Lilly. She has received consulting fees from the Simon Foundation and Cura Sen, Inc. She serves as associate editor for Frontiers in Aging Neurosciences, Frontiers in Dementia and the Journal of Alzheimer Disease. G.D.R. receives research support from NIH, Alzheimer's Association, American College of Radiology, Tau Research Consortium, Avid Radiopharmaceuticals, Eli Lilly, GE Healthcare, Life Molecular Imaging. He has served as a consultant for Eisai, Merck, Axon Neurosciences. He received speaking honoraria from GE Healthcare. He serves as Associate Editor for JAMA Neurology. J.C.R. is a site PI for clinical trials supported by Eli Lilly and receives support from NIH. A.L.B. receives research support from NIH, the Tau Research Consortium, the Association for Frontotemporal Degeneration, Bluefield Project to Cure Frontotemporal Dementia, Corticobasal Degeneration Solutions, the Alzheimer's Drug Discovery Foundation and the Alzheimer's Association. He has served as a consultant for Aeton, Abbvie, Alector, AGTC, Amgen, Arkuda, Arvinas, Asceneuron, Ionis, Lundbeck, Novartis, Passage BIO, Sangamo, Samumed, Third Rock, Toyama and UCB, and received research support from Avid, Biogen, BMS, C2N, Cortice, Eli Lilly, Forum, Genentech, Janssen, Novartis, Pfizer, Roche and TauRx.

The Netherlands [3]Eli Lilly and Company, Indianapolis, Indiana, United States of America [4]Institute of Neuroscience and Physiology, Department of Psychiatry and Neurochemistry, the Sahlgrenska Academy at the University of Gothenburg, Mölndal, Sweden [5]Clinical Neurochemistry Laboratory, Sahlgrenska University Hospital, Mölndal, Sweden [6]Department of Neurodegenerative Disease, UCL Institute of Neurology, Queen Square, London, United Kingdom [7]UK Dementia Research Institute at UCL, London, United Kingdom [8]Department of Pathology, University of California, San Francisco, California, United States of America [9]Department of Neurology, Mayo Clinic, Rochester, Minnesota, United States of America [10]Department of Radiology & Biomedical Imaging, University of California, San Francisco, California, United States of America

Abstract

With the potential development of new disease-modifying Alzheimer's Disease (AD) therapies, simple, widely available screening tests are needed to identify which individuals who are experiencing symptoms of cognitive or behavioral decline should be further evaluated for initiation of treatment. A blood-based test for AD would be a less invasive and less expensive screening tool than the currently approved CSF or amyloid β-PET diagnostic tests. We examined whether plasma phosphorylated tau at residue 181 (pTau181) could differentiate between clinically diagnosed or autopsy confirmed AD and Frontotemporal Lobar Degeneration (FTLD). Plasma pTau181 concentrations were increased by 3.5 fold in AD compared to controls and differentiated AD from both clinically diagnosed (Receiver Operating Characteristic Area Under the Curve [AUC]=0.894) and autopsy confirmed FTLD (AUC=0.878). Plasma pTau181 identified amyloid β-PET positive individuals regardless of clinical diagnosis and correlated with cortical tau protein deposition measured by ^{18}F-Flortaucipir PET. Plasma pTau181 may be useful to screen for tau pathology associated with AD.

Introduction

With the potential development of new disease modifying treatments for Alzheimer's disease (AD),[1] screening tests that can be widely and inexpensively deployed to identify those who might benefit from treatment are urgently needed. Particularly important will be differentiating AD from other related dementias, such as frontotemporal lobar degeneration (FTLD), that can sometimes be misdiagnosed as AD in younger individuals or patients with mild or questionable symptoms, called Mild Cognitive Impairment (MCI). Currently, two technologies are approved for differential diagnosis of AD from other dementias, expert interpretation (visual read) of measurements of brain beta-amyloid (Aβ) deposition with Aβ positron emission tomography (Aβ-PET)[2] or Aβ and tau measurements in cerebrospinal fluid (CSF).[3,4] These biomarkers are not widely used because of the invasiveness of lumbar punctures required for obtaining CSF and the high costs of PET imaging, often not reimbursed by third-party payers.[2] Moreover, PET scans are associated with exposure to radiation and access to PET imaging is often restricted to specialized centers. A blood-based test for AD would be a less invasive and less expensive screening tool to identify individuals who are experiencing symptoms of cognitive or behavioral decline and might benefit from

more comprehensive CSF or PET testing for diagnostic purposes or prior to initiation of a disease modifying AD therapy.

Examining the performance of a screening diagnostic test for AD in FTLD patients is important because FTLD is similarly prevalent to AD in individuals who are less than 65 years at onset and can be difficult to differentiate from AD because of similar clinical features such as language and executive function impairments.[5] Moreover, at autopsy, insoluble tau deposition is present in both neuropathologically diagnosed AD (AD_{path}) and a subset of FTLD syndromes (FTLD-tau), including approximately half of behavioral variant frontotemporal dementia (bvFTD), most nonfluent variant primary progressive aphasia (nfvPPA) and almost all progressive supranuclear palsy (PSP) patients.[6] Whereas in AD_{path}, tau pathology is associated with elevated concentrations of CSF tau species, including (total) tau and phosphorylated tau at residue 181 (pTau181)[7,8] in FTLD, CSF tau and pTau181 can be either elevated or decreased.[9] Insoluble tau deposition can be visualized in the brains of living AD individuals using Flortaucipir (FTP)-PET, a tracer which binds with high affinity to mixed 3 and 4 microtubule binding domain repeat (3R/4R) tau that is found in AD_{path} neurofibrillary tangles,[10] and can distinguish clinical AD (AD_{clin}) from other diseases.[11] However, FTP has low affinity for the predominantly 3R- or 4R tau deposits found in most FTLD, limiting its usefulness.[9] In contrast, levels of neurofilament light chain (NfL) a marker of axonal damage measurable in CSF, plasma and serum[12-14] are increased in FTLD and correlate with survival,[15] clinical severity and brain volume.[16-19] CSF and serum NfL concentrations are also elevated in AD_{clin}, but less so than in FTLD.[13,17,20,21] As in FTLD, serum NfL is predictive of cortical thinning and rate of disease progression in AD_{clin}.[22,23]

Recent studies have shown that Aβ42/40 ratio measured in plasma can differentiate between normal controls and AD patients using immunoprecipitation-mass spectrometry (IP-MS), but this technology is not accessible to most clinical laboratories.[24-26] Novel ultrasensitive single molecule array (Simoa) antibody based approaches measuring Aβ in blood are easier to implement but do not yet have sufficient diagnostic precision to be useful clinically.[26] Elevated levels of total tau measured with Simoa technology in plasma are associated with cognitive decline[27] although there is substantial overlap between concentrations measured in normal aging and AD limiting the diagnostic usefulness of such assays.[28-30]

Recently, a new plasma pTau181 assay was found to differentiate AD_{clin} from healthy controls.[31] We tested the differential diagnostic ability of these plasma pTau181 measurements to differentiate MCI and AD_{clin} relative to a variety of clinical FTLD phenotypes. A subset of diagnoses was verified using neuropathological examination at autopsy or by the presence of autosomal dominant mutations that lead to specific types of FTLD pathology, including mutations in the tau gene (*MAPT*) that lead to FTLD pure 4R tau or AD-like mixed 3R/4R tau deposition in the brain. We also compared plasma pTau181 to the current clinical standards for dementia differential diagnosis, Aβ-PET and CSF pTau181, as well as to the research biomarkers plasma NfL, plasma Aβ 42 and 40, FTP-PET and brain atrophy measured with MRI, to better evaluate the biological basis for elevated plasma pTau181.

Results

Participant characteristics

Baseline demographics, clinical assessments, imaging measures, and fluid biomarker levels are shown in Table 1. The control group (NC) and the MCI group were younger than the PSP and nfvPPA groups. Plasma pTau181 and NfL concentrations were similar in men and women. Plasma NfL concentrations correlated with age (ρ=0.19, p=0.006) and with time between blood draw and death in autopsy cases (ρ=−0.27, p=0.009); pTau181 concentrations were not correlated with either value. Plasma pTau181 concentrations were associated with the Clinical Dementia Rating Scale® sum of boxes score (CDRsb; β=0.184, p=0.004, supplementary Table 1), as were NfL concentrations (β=0.456, p<0.0001, supplementary Table 2). FTP-PET binding was highest in AD_{clin} cases, compared to MCI, CBS, PSP, bvFTD, and nfvPPA. Pittsburgh Compound B (PiB) Aβ-PET binding was highest in AD_{clin}. 27% of controls were Aβ-PET positive (visual read). CSF pTau181 was higher in AD_{clin} compared to every other diagnosis except for MCI and svPPA.

Plasma pTau181 and NfL comparisons by clinical diagnostic group

Plasma pTau181 concentrations were elevated in AD_{clin} compared to all other groups (Figure 1A, Table 1). Plasma NfL concentrations were elevated in CBS, PSP, and bvFTD compared to AD_{clin} and MCI as well as controls (Figure 1B). NfL concentrations were also elevated in nfvPPA and svPPA as compared to controls and MCI. NfL was increased in AD compared to NC. The ratio of pTau181/NfL was decreased in all FTLD diagnoses compared to controls, AD_{clin} and MCI patients (extended data Figure 1). The AD-associated lvPPA cases had increased pTau181 levels compared to the FTLD-associated nfvPPA, svPPA and controls (Figure 1C). An age-adjusted plasma pTau181 cut-off of 8.7 pg/mL differentiated AD_{clin} from $FTLD_{clin}$ with a ROC area under the curve (AUC) of 0.894 (p<0.0001, Figure 1D, Table 2). The plasma Aβ 42/40 ratio did not differ between the clinical diagnostic groups (extended data Figure 2A), but was able to differentiate between Aβ-PET positive and negative cases (AUC=0.768, p<0.0001, extended data Figure 2B, Table 2), and FTP-PET positive and negative cases (AUC=0.782, p<0.0001, extended data Figure 2C, Table 2).

Plasma pTau181 and NfL in pathology-confirmed cases and FTLD mutation carriers

Neuropathological diagnosis was available in 82 cases. Due to potential effects of disease severity, analyses were adjusted for age and CDRsb at time of blood draw. Median plasma pTau181 concentrations were higher in AD_{path} (n=15, 7.5±8 pg/mL) compared to FTLD-tau (n=52, 2.3±3 pg/mL, p<0.0001) and FTLD-TDP (n=15, 2.1±2 pg/mL, p<0.0001, Figure 2A). Plasma pTau181 differentiated AD_{path} from the combined FTLD-TDP and FTLD-tau group (AUC=0.878, p<0.0001, Figure 2B), from FTLD-TDP alone (AUC=0.947, p<0.0001) and from FTLD-tau alone (AUC=0.858, p<0.0001, Table 2). Plasma NfL was a poor discriminator of AD_{path} from $FTLD_{path}$ (Table 2). pTau181 was associated with autopsy defined Braak stage (β=0.569, p<0.0001) and was higher in Braak stage 5-6 (n=16, 4.9±4 pg/mL) compared to Braak 0 (n=10, 2.1±2 pg/mL, p=0.003), Braak 1-2 (n=42, 2.2±2 pg/mL, p<0.0001), and Braak 3-4 (n=13, 2.3 ±3pg/mL, p=0.009, Figure 2C). NfL did not differ by Braak stage (extended data Figure 3).

Seventy-six individuals were FTLD-causing mutation carriers (61 *MAPT*, 5 *GRN*, 10 *C9orf72*). There was no difference in pTau181 concentrations between the mutation carriers (grouped by mutated gene) or the mutation carrier groups and normal controls (extended data Figure 4). Plasma pTau levels were increased in *MAPT* mutation carriers with AD-like mixed 3R/4R tau pathology (n=17, 4.4±4 pg/mL, Figure 2D), compared to those with pure 4R tau pathology[32] (n=44, 2.2±2 pg/mL, p=0.024), and controls (n=44, 2.0±2 pg/mL, p=0.011). Plasma pTau181 differentiated AD_{path} from $FTLD_{path}$ and mutation carriers combined (AUC=0.854, p<0.0001, Table 2).

Association between plasma pTau181 and other fluid biomarkers

Plasma pTau181 and plasma NfL concentrations were associated in the combined AD_{clin} and MCI cases (β=0.66, p<0.0001, Figure 3A), but not in the whole patient sample. CSF pTau181 was associated with plasma pTau181 in the whole sample (β=0.51, p<0.0001; n=74, extended data Figure 5), and both within the AD/MCI (β=0.41, p=0.042; n=25), and the FTLD group (β=0.49, p<0.0001; n=29), but not in controls. CSF pTau181 concentrations were higher in AD_{clin} (45.8±31 pg/mL), compared to FTLD (22.1±8 pg/mL, p<0.0001) and differentiated the two clinical diagnoses (AUC=0.931, p<0.0001, Table 1, Table 2).

Plasma pTau181 and NfL associations with tau (FTP)-PET and Aβ-PET

There were strong linear relationships between plasma pTau181 concentrations and PiB-SUVR (β=0.75, p<0.0001, Figure 3B) as well as global cortical FTP SUVR (β=0.73, p<0.0001, Figure 3C). Plasma NfL concentration was not related to either PET measure. An age-corrected plasma pTau181 cut-off for Aβ-PET positivity of 8.0 pg/mL discriminated between all Aβ-PET positive and negative individuals with 0.889 sensitivity, 0.853 specificity and AUC 0.914 (p<0.0001, Figure 3D and Table 2). Plasma pTau181 also differentiated between Aβ-PET positive and negative cases within the healthy controls and MCI groups individually. In controls, the AUC was 0.859 (p<0.0001, 11 Aβ-PET positive, 29 negative). Within the MCI group, the AUC was 0.944 (p<0.0001, 18 Aβ-PET positive, 21 negative, Table 2, extended data Figure 6).

When a cortical FTP-SUVR diagnostic threshold[33] of 1.22 was applied to designate all cases as FTP-PET positive and negative, plasma pTau181 was also a good discriminator of FTP-PET status (AUC=0.919, p<0.0001, Figure 3E). In the MCI cases alone, the AUC for FTP-PET status was 0.977 (p<0.0001, 11 FTP-PET positive, 20 negative, Table 2). Similar relationships between plasma pTau181 and FTP-PET were obtained with the independent cohort from an Eli Lilly AD_{clin}/MCI clinical research study (n=42; Supplementary Results, supplementary Table 3). Plasma NfL did not differentiate between Aβ-PET positive and negative cases (AUC = 0.559, p=0.276) or between FTP-PET positive and negative cases (AUC = 0.606, p=0.159, Table 2). pTau181 was associated with FTP-PET-estimated Braak stage[9,34,35] (β=0.610, p<0.0001) and was higher in FTP-PET Braak stage 5-6 (n=54, 9.2±4 pg/mL) and Braak stage 3-4 (n=8, 6.4±3 pg/mL) compared to Braak 0 (n=26, 2.4±2 pg/mL, both p<0.0001). NfL did not differ by FTP-estimated Braak stage (extended data Figure 7).

Voxelwise analyses of FTP-PET and grey matter volume in relation to plasma pTau181 and NfL

pTau181 concentrations were strongly associated with FTP-PET SUVR values (Spearman's ρ values exceeding 0.70 in peak regions) in the frontal, temporoparietal, and posterior cingulate cortices, and precuneus regions (Figure 4A). Associations remained significant in the AD_{clin}/MCI patients only, although with slightly lower ρ values. There were insufficient data to perform the analyses in the FTLD group separately (n=18). There was no association between NfL concentrations and FTP-PET uptake in the whole group. In the AD_{clin}/MCI patients only there were weak correlations in the right hemisphere that did not survive multiple comparisons corrections, predominantly in the frontal and insular cortex, and in the right temporal horn (reaching ρ~0.6 in the insula; Figure 4A).

High plasma pTau181 concentrations correlated with lower grey matter volume in the bilateral medial temporal lobe, the posterior cingulate cortex and precuneus (ρ=−0.35, p<0.001, Figure 4B). This association was driven by the AD_{cin}/MCI cases, who showed the highest correlation coefficients in these regions (ρ=−0.55, p<0.001). There was no association between plasma pTau181 and grey matter volume in FTLD cases. In the combined group there were strong negative correlations between NfL and grey matter volume in the right putamen and insula (ρ~−0.5, p<0.001), and to a lesser extent with grey matter volume in the medial prefrontal cortices (ρ~−0.45, p<0.001). In the FTLD group, the association was maximal in the right putamen and insula (ρ~−0.4, p<0.001), with lower correlations present in the frontal and lateral temporal regions, and right precuneus (Figure 4B).

Plasma pTau181 and NfL associations with clinical disease severity and cognitive function

pTau181 showed strong associations with baseline CDRsb scores (β=0.486, p<0.0001), functional activities questionnaire (FAQ) (β=0.541, p<0.0001) and modified Rey figure recall (β=−0.585, p<0.0001) only in the AD_{clin}/MCI group and not in the control or FTLD groups. In contrast, NfL showed associations with CDRsb and neuropsychological performance in both the AD_{clin}/MCI and FTLD groups (β=0.472, p<0.0001 for CDRsb in AD_{clin}/MCI; β=0.244, p<0.010 in FTLD; supplementary Table 1 and supplementary Table 2). In longitudinal analyses, higher baseline pTau181 was associated with faster rates of decline in AD_{clin}/MCI patients in CDRsb, MMSE, Rey recall, Boston Naming Test (BNT), and FAQ (supplementary Table 4), whereas higher baseline NfL predicted faster decline over time in FTLD patients in MMSE, phonemic fluency and trail making test (supplementary Table 5).

Discussion

The main findings of this study are that plasma pTau181 concentrations differentiated clinically diagnosed AD patients from FTLD patients and elderly controls, and that plasma pTau181 concentrations were strongly associated with currently approved AD-biomarker measurements including Aβ-PET and CSF pTau181, regardless of clinical diagnosis. Plasma pTau181 also differentiated autopsy-diagnosed AD from FTLD with slightly lower accuracy than clinically-diagnosed or PET-defined cases. Plasma pTau181 accurately identified

elderly controls and MCI individuals with a positive Aβ-PET scan suggesting underlying AD_{path} changes and also differentiated between individuals with elevated cortical tau deposition measured by FTP-PET. Elevated pTau181 concentrations correlated with higher FTP-PET uptake, and more severe grey matter atrophy in AD-related brain regions. Plasma pTau181 reflected severity of cortical AD tau pathology as reflected by Braak stage measured at autopsy.[11,36] Plasma pTau181 also predicted the rate of decline on clinical measures of disease severity and neuropsychological status over two years of follow up in AD_{clin}/MCI. These findings were specifically related to plasma pTau181 since plasma concentrations of NfL, a nonspecific biomarker of neurodegeneration, were not related to AD diagnosis, Aβ- or FTP-PET signal. As expected, NfL concentrations were associated with measures of disease severity, cognitive function and grey matter atrophy most strongly in FTLD patients.[37] Together, these data suggest that plasma pTau181 may be a useful screening tool for identifying the AD pathobiological process in individuals at risk for cognitive decline or with cognitive impairment.

Aβ-PET has established clinical utility for differential diagnosis of AD_{clin} from other dementias, is associated with more severe clinical and cognitive decline,[38] and has been validated as a measure of AD neuropathology.[39,40] Plasma pTau181 accurately differentiated between AD and FTLD, similar to the previously reported diagnostic accuracy of Aβ-PET.[41] This suggests that the diagnostic value of plasma pTau181 could be comparable to Aβ-PET in patients who are symptomatic with MCI or dementia. We found that increased plasma pTau181 concentrations were associated with Aβ-PET positivity even in cognitively normal controls, however plasma pTau181 is unlikely to be a direct measure of Aβ pathology. Others have found that there is often significant tau accumulation in Aβ-PET positive healthy elderly controls, suggesting that amyloid positivity is a hallmark for Alzheimer pathology and may reflect not only amyloid, but also pre-symptomatic tau accumulation.[42] As plasma pTau181 was related to regional tau deposition measured by Braak stage at autopsy or estimated by FTP-PET uptake during life, this might explain the ability of pTau181 to differentiate between Aβ-PET positive and negative controls. A limitation of our study was that we had few data from healthy controls with FTP-PET data, and so we could not directly test the relationship of pTau181 to FTP-PET status in these individuals.

Whereas CSF total tau has little diagnostic value differentiating FTLD from AD,[43] CSF pTau181 is able to differentiate clinically diagnosed AD from FTLD with a sensitivity and specificity of approximately 70-80%[44,45] which is similar to the accuracy found in this study using plasma pTau181. Using autopsy data, we determined a specific association of elevated plasma pTau181 with underlying mixed 3R/4R tau pathology that is characteristic of, but not specific to AD. We found elevated pTau181 concentrations in AD_{path}, which is known to have neurofibrillary tangles consisting of 3R/4R mixed tau pathology, and low pTau181 concentrations in sporadic FTLD-tau which is associated with insoluble deposits of either 3R (eg., Pick's disease) or 4R tau (eg., Corticobasal Degeneration or Progressive Supranuclear Palsy) pathology. To test the hypothesis that plasma pTau181 concentrations specifically reflect mixed 3R/4R tau pathology we measured samples from individuals with rare *MAPT* mutations (R406W and V337M)[32,46,47] that lead to FTLD pathology with accumulation of neurofibrillary tangles consisting of 3R/4R tau that are similar to those seen in AD_{path} that often cause a clinical syndrome similar to AD_{clin} but notably without Aβ

pathology. Individuals with *MAPT* mutations that lead to 3R/4R tau pathology had elevated plasma pTau181 concentrations compared to individuals with other *MAPT* mutations that lead to pure 4R tau pathology (eg. P301L) and healthy controls. While this may be of interest mechanistically, this is unlikely to affect the utility of plasma pTau181 as an AD screening diagnostic test because *MAPT* R406W and V337M mutations are exceedingly rare, and overall plasma pTau181 levels were lower in these individuals than in AD patients. Together, these results suggest that both CSF and plasma pTau181 reflect 3R/4R tau accumulation in the brain that is usually associated with AD pathology.

Plasma pTau181 concentrations were correlated with regional FTP-PET uptake which is thought to reflect AD neurofibrillary tangle deposition.[11,48,49] Supportive of this hypothesis, we found an association between plasma pTau181 and estimated Braak stage by FTP-PET as well as with neuropathological Braak stage. The association of pTau181 with FTP-PET was stronger than with neuropathological Braak staging. Even though plasma pTau181 could differentiate late stage tau pathology (Braak 5-6) from other stages, it could not differentiate early and moderate stages (Braak 1-2 and 3-4) from the group without pathology (Braak 0). This could indicate a limitation in the sensitivity of plasma pTau181 for AD pathology, but could also reflect differences in sample size, the more comprehensive anatomical coverage with PET and additional variability introduced by the delay from blood draw to autopsy in the pathological Braak stage analysis that was not present in the FTP-PET Braak stage analysis.[50] The increased pTau181 concentrations in AD_{clin} and their strong association with AD patterns of brain atrophy suggests that plasma pTau181 is also associated with AD-related neuronal loss. More detailed comparisons of neuronal cell loss measured by neuropathology and plasma pTau181 concentration will be necessary to test this hypothesis.

Plasma Aβ measured on an automated platform has recently been demonstrated as a promising and cost-effective tool as compared to Aβ-PET, to identify brain amyloidosis in individuals with or at risk for AD.[51] We found that the fold change in mean plasma pTau181 concentration between Aβ-PET positive and negative individuals in our study exceeded the fold change found by others using plasma Aβ42/40 ratio and the overlap between groups seemed much smaller.[24-26,51] Although we did not have access to the same automated Aβ measurement platform or to IP-MS, we measured plasma Aβ42/40 by Simoa and found a much larger fold difference in pTau181 between groups as compared to Aβ42/40. Aβ42/40 concentrations were less accurate in differentiating between Aβ-PET positive and negative individuals than pTau181. Future comparisons with more accurate plasma amyloid tests will be necessary to determine the relative value of plasma amyloid as compared to pTau181 measurements.

This study has a number of important limitations. There were several outlier high plasma pTau181 values in the clinical diagnostic groups who were not expected to have elevated pTau181: two controls, one in CBS, PSP, bvFTD, nfvPPA, and svPPA. These findings may reflect previously undetected brain 3R/4R tau deposition. In support of this interpretation, one of those controls was Aβ-PET positive, the CBS case had unknown amyloid status and could have had AD pathology,[52] the PSP case had autopsy data showing AD co-pathology, and the bvFTD case was a *MAPT* mutation carrier, associated with tau pathology. We also had fewer AD_{path} cases than autopsy confirmed FTLD-tau cases, which might have

influenced the results. Verification of the diagnostic performance of plasma pTau181 in a larger number of autopsy confirmed cases will be important. We had little FTP-PET data in healthy controls and FTLD cases, therefore we were not able to examine voxelwise associations with pTau181 in these individuals. Having pre-symptomatic Aβ-PET positive and Aβ-PET negative cases with high pTau181 levels and FTP-PET imagining would help to determine whether pTau181 associates primarily with FTP-PET or Aβ-PET. The sample sizes were balanced by clinical diagnosis, but more were in the FTLD spectrum. A larger number of controls, MCI patients and AD patients would have offset this, though accuracy of pTau181 in these groups has been demonstrated in a previous study.[31] Finally, neither plasma pTau181 nor NfL were able to differentiate between autopsy confirmed FTLD-tau and FTLD-TDP cases. More work will be necessary to identify effective biomarkers for this context of use.

This study provides strong evidence that plasma pTau181 concentration could be a useful screening blood test to identify underlying mixed 3R/4R tau pathology consistent with AD in individuals who have symptoms of cognitive or behavioral decline in clinical settings where diagnostic status may be uncertain. Since Aβ-PET scans are expensive and require specialized imaging centers, plasma pTau181 may be a more readily accessible tool to identify individuals who should undergo more detailed diagnostic testing with this approved technology. Alternatively, given the strong relationship between plasma pTau181 and FTP-PET uptake, plasma pTau181 could be useful as a screening tool in clinical trials employing this FTP-PET to measure treatment effects of novel AD therapies.

Methods

Participants

This retrospective study included 404 participants from three independent cohorts (Table 1, supplementary Table 3), a primary cohort of 362 cases; 301 cases from the University of California San Francisco (UCSF) Memory and Aging Center and 61 from the Advancing Research and Treatment for Frontotemporal Lobar Degeneration (ARTFL) consortium, and a secondary cohort of baseline data from 42 participants in an Eli Lilly sponsored research study (www.clinicaltrials.gov: NCT02624778). Participants were only included in the study when their plasma pTau181 measurement was successful. Aβ-PET was available in 226 participants, 138 had FTP-PET (79AD_{clin}/MCI and 18 FTLD in the primary cohort, 41 AD_{clin}/MCI secondary cohort), 220 participants had MRI (71 AD_{clin}/MCI, 110 FTLD, 39 NC), and 74 cases had previous CSF pTau181 concentrations available (20 NC, 25 AD_{clin}/MCI, 29 FTLD, average time between plasma and CSF sample was 1.3±2 years). The primary cohort consisted of 362 cases; 70 normal controls, 103 cases in the AD spectrum: 56 AD_{clin} per NIA-AA criteria[53] including 14 logopenic variant PPA (lvPPA) and 47 MCI,[54] and 190 patients meeting clinical criteria for a syndrome in the FTLD spectrum: 39 corticobasal syndrome (CBS)[52], 48 PSP,[55] 50 bvFTD,[56] 27 nonfluent variant PPA (nfvPPA) and 26 semantic variant PPA individuals (svPPA).[57] These included 76 carriers of FTLD-causing mutations: 61 microtubule associated protein (*MAPT*), five progranulin (*GRN*) and ten chromosome 9 open reading frame 72 *(C9orf72)*. The *MAPT* mutation carriers group included 17 individuals with mutations that produce 3R/4R tau (10 V337M and 7 R406W),

and 44 with mutations that produce 4R tau (22 P301L, 11 N279K, 4 IVS9-10G>T, 3 IVS10+16C>T, 1 S305S, 1 S305I, and 2 S305N).[32]

All AD cases and 38 of the 47 MCI cases had either Aβ-PET, MRI, autopsy or genetic biomarker verification. 82 cases had an autopsy-confirmed diagnosis: 15 AD_{path}, 52 FTLD-Tau and 15 FTLD-TAR DNA-binding protein 43 (FTLD-TDP). The average time between blood draw and death in these cases was 2.7±2 years. Normal controls were healthy elderly with normal neurological examinations, neuropsychological testing and Clinical Dementia Rating (CDR®)[58] scores. Longitudinal measures of disease severity, neuropsychological testing and executive function were available at baseline and two follow-up visits (average n baseline = 221, time point two = 115 cases, time point three = 40 cases) with an average 1.2±0.1 years between measurements. Participants provided written informed consent at the time of recruitment. The study was approved by the institutional review board of each research center from which the individual was recruited.

Clinical evaluation

Disease severity was assessed using the CDR® scale sum of boxes (CDRsb),[58] and Mini-Mental State Exam (MMSE).[59] Neuropsychological measures included a Trail-Making test,[60] Color Trails test,[61] phonemic fluency,[62] the Boston Naming Test (BNT),[63] Modified Rey Figure copy and recall,[60] and Geriatric Depression Scale (GDS).[64] Disability was assessed using the Functional Activities Questionnaire (FAQ),[65] and the Schwab and England Activities of Daily Living (SEADL) scale.[66]

Statistical analysis

A two-sided $p<0.05$ was considered statistically significant and corrected for multiple comparisons using false discovery rate when appropriate.[67] Biomarker concentrations were not normally distributed and natural log-transformed data or non-parametric statistics were used. Differences in biomarker values and in clinical and neuroimaging variables were assessed with one-way ANOVA or Kruskal-Wallis tests, with Bonferroni multiple-comparisons correction. Associations between pTau181 and NfL concentrations, FTP-PET cortical SUVR values, PIB-PET cortical SUVR values and clinical measures were assessed using linear regression models, corrected for false discovery rate.[67] Receiver operating characteristic (ROC) analyses determined the ability of plasma pTau181 and NfL to differentiate between diagnostic groups. Youden cut-off values were used for sensitivity and specificity.[68] All analyses were corrected for age, CDRsb, and time between blood draw and death as appropriate. There were no differences in plasma biomarker levels between sexes. Linear mixed effect models evaluated the relationship of baseline ln pTau181 with changes in clinical variables. Models allowed random intercepts at the subject level and were adjusted for age, sex, time differences from specimen collection date to clinical/neuropsychological testing, disease duration, and biomarker by time interaction. Statistical analyses were performed using SPSS (version 25; SPSS/IBM, Chicago, IL), Stata (Stata 14.0, StataCorp LLC) and R (version 3.5.1).

Fluid biomarker methods

Plasma pTau181 measurements

Blood samples were obtained by venipuncture in ethylenediaminetetraacetic acid (EDTA) tubes for plasma, following the ADNI protocol.[69] Within 60 minutes, the samples were centrifuged at 3000 rpm at room temperature, aliquoted and stored at −80°C. Plasma pTau181 levels were measured in duplicate by electrochemiluminescence using a proprietary pTau181 assay (Lilly Research Laboratory, Indianapolis, IN) as previously described.[31] Briefly, samples were diluted 1:2 and 50 μL of diluted sample was used for the assay. The assay was performed on a streptavidin small spot plate using the Meso Scale Discovery (MSD) platform. Biotinylated-AT270 was used as a capture antibody (anti-pTau181 Tau antibody, mouse IgG1) and SULFO-TAG-Ru-LRL (anti-tau monoclonal antibodies developed by Lilly Research Laboratory) for the detector. The assay was calibrated using a recombinant tau (4R2N) protein that was phosphorylated in vitro using a reaction with glycogen synthase kinase-3 and characterized by mass spectrometry.

41 of the included samples were measured below the lower limit of quantification (LLOQ) of 1.4 pg/mL, none of which in the AD phenotype. One sample from an Aβ-PET negative normal control had a pTau181 concentration of 49.1 pg/mL, almost 12 times as high as the average pTau181 value. This case was excluded from all analyses. The average %CV of the samples was 7.3%. The %CV of the low quality control was 5.6% and 4.6% for the high quality control.

Plasma NfL measurements

Plasma NfL concentrations were measured at three sites; Novartis Institutes for Biomedical Research, Quanterix Corp (Boston, MA), and UCSF using a commercially available NfL kit on the Simoa HD-1 platform. Samples were 4x diluted, automated by the HD-1 analyzer and measured in duplicate. The average interassay variation was 4.9%, all samples were measured well above the kit LLOQ of 0.174 pg/mL. One sample had an NfL concentration of 713 pg/mL, almost 20 times as high as the average NfL value. This value was excluded from all analyses.

In a previous study, with an overlapping set of samples from 186 participants were analyzed separately at Novartis and at Quanterix, showing that plasma NfL concentrations were highly correlated ($\rho = 0.98$, $p < .001$). The samples analyzed at the two sites also had comparable means and standard deviations (21.8 ± 35 pg/mL, Quanterix and 20.2 ± 34 pg/mL, Novartis).

Plasma Aβ42 and Aβ40 measurements

Plasma Aβ42 and 40 was measured at UCSF using the Neurology 3-plex A kit from Quanterix, that measures Aβ42, Aβ40 and tau. Samples were 4x diluted, automated by the HD-1 analyzer and measured in duplicate. The average interassay variation was 6.4% for Aβ42 and 2.9% , all samples were measured well above the kit LLOQ of 0.142 pg/mL for Aβ42 and 0.675 for Aβ40.

CSF pTau181 measurements

CSF pTau181 was measured in duplicate with the INNO-BIA AlzBio3 (Fujirebio, Gent, Belgium) platform by a centralized laboratory.

The researchers performing the fluid biomarker analyses were blinded to the clinical information and reference standard results of the participants during sample measurement.

Imaging methods

MRI acquisition

Structural MRIs were available for 221 participants and acquired at UCSF on a 3T Siemens Tim Trio or a 3T Siemens Prisma Fit scanner at an average of 20 (±58) days from the plasma sample. T1-weighted magnetization prepared rapid gradient echo (MPRAGE) MRI sequences were acquired at UCSF, either on a 3T Siemens Tim Trio or a 3T Siemens Prisma Fit scanner. Both scanners had similar acquisition parameters on each scanner (sagittal slice orientation; slice thickness = 1.0 mm; slices per slab = 160; in-plane resolution = 1.0x1.0 mm; matrix = 240x256; repetition time = 2,300 ms; inversion time = 900 ms; flip angle = 9°), although echo time slightly differed (Trio: 2.98 ms; Prisma: 2.9ms).

MRI preprocessing

Before pre-possessing, all scans were visually inspected for quality control. Images with excessive motion or image artifact were excluded. T1-weighted images underwent bias field correction using an N3 algorithm and segmentation was performed using Statistical Parametric Mapping (SPM12; Wellcome Trust Center for Neuroimaging, London, UK, http://www.fil.ion.ucl.ac.uk/spm) unified segmentation.[70] The Total Intracranial Volume (TIV)[71] was derived from SPM12 to be used in statistical analyses. A group template was generated from the segmented gray and white matter tissues and cerebrospinal fluid by non-linear registration template generation using the Large Deformation Diffeomorphic Metric Mapping framework.[72] Native subject space gray were normalized, modulated and smoothed in group template space with a 10mm full width half maximum Gaussian kernel. Every step of the transformation from the native space to the group template was carefully inspected.

FTP-PET acquisition

FTP-PET was acquired on a Siemens Biograph PET/CT scanner at the Lawrence Berkeley National Laboratory (LBNL) for 75 participants (65 AD/MCI and 10 FTLD) at an average of 70 (±122) days from the plasma sample. FTP was synthesized and radiolabeled at LBNL's Biomedical Isotope Facility. We analyzed PET data that was acquired 80–100 min after the injection of ~10 mCi of FTP (four 5-min frames). A low-dose CT scan was performed for attenuation correction prior to PET acquisition, and data were reconstructed using an ordered subset expectation maximization algorithm with weighted attenuation and smoothed with a 4 mm Gaussian kernel with scatter correction (image resolution: 6.5 x 6.5 x 7.25 mm based on Hoffman phantom).

FTP-PET preprocessing

PET frames were realigned, averaged and coregistered onto their corresponding T1-MRI. Standardized Uptake Value Ratio (SUVR) images were created using the inferior cerebellum gray matter as a reference region (the region was defined using the T1-MRI was segmented using Freesurfer 5.3 (http://surfer.nmr.mgh.harvard) and SPM12.[33] Native-space FTP-SUVR images were warped to template space using the deformation parameters derived from the MRI procedure. Warped SUVR images were masked to limit contamination from non-relevant areas (eg. off-target binding from meninges, eyes or skull) and smoothed with a 4mm isotropic Gaussian kernel to be used for voxelwise analyses.[48]

FTP-PET analyses

Using Freesurfer segmentation, the average cortical SUVR value was extracted from each patient in native space to have a measure of global tau burden.[48] Patients were categorized as “tau-positive” or “tau-negative” based on a previously published cortical FTP-SUVR threshold of 1.22 (see Table 3 from Maass et al[33]). Complementary analyses were conducted using inferior temporal lobe SUVR values to classify patients (using a 1.30 threshold, see Table 3 from Maass et al[33]) but results were unchanged.

Patients were assigned to a Braak stage (0, I-II, III-IV or V-VI) using the approach developed by Maass et al.[33] For each patient, we extracted the average SUVR from 3 bilateral composite regions of interest (ROIs) in native space based on Freesurfer 5.3’s aparc +aseg segmentation file, as follows:

Braak I-II ROI: entorhinal, hippocampus.

Braak III-IV ROI: parahippocampal, fusiform, lingual, amygdala, middle temporal, caudal anterior cingulate, rostral anterior cingulate, posterior cingulate, isthmus cingulate, insula, inferior temporal, temporal pole.

Braak V-VI ROI: superior frontal, lateral orbitofrontal, medial orbitofrontal, frontal pole, caudal middle frontal, rostral middle frontal, pars opercularis, pars orbitalis, pars triangularis, lateral occipital, supramarginal, inferior parietal, superior temporal, superior parietal, precuneus, banks of the superior temporal sulcus, transverse temporal, pericalcarine, postcentral, cuneus, precentral, paracentral.

The Braak stage classification scheme (including thresholds) was determined in Maass et al[33] and works as follows:

Step 1. If average SUVR in Braak V-VI ROI > 1.25, participant is assigned to Braak stage V-VI; if not:

Step 2. If average SUVR in Braak III-IV ROI > 1.28, participant is assigned to Braak stage III-IV; if not:

Step 3. If average SUVR in Braak I-II ROI > 1.35, participant is assigned to Braak stage I-II; if not, participant is assigned to Braak stage 0.

FTP-PET imaging in secondary cohort (Eli Lilly)

The tau PET acquisitions were performed from 75 to 105 minutes (6 x 5 min frames) after injection of approximately 240 MBq of FTP. Frames were aligned and averaged with an acquisition time-offset correction. Average 75-105 min image was spatially registered to the corresponding individual subject's MRI space and then to the MRI template in Montreal Neurological Institute (MNI) stereotaxic space. Reference signal was parametrically derived in the white matter-based region to isolate non-specific signal using the parametric estimate of reference signal intensity (PERSI) method.[73] The used weighted SUVR was designed by multiblock barycentric discriminant analysis (MUBADA) that has been shown to maximize the separation of diagnostic groups and amyloid status.[74]

Aβ-PET

Aβ status was available for 166 participants (41 NC, 77 AD/MCI, 48 FTLD) and derived from PET acquired with 11C-Pittsburg Compound B (PIB, injected dose: ~15 mCi; n=124 participants) or 18F-Florbetapir (injected dose: ~10 mCi; n=42) at an average of 273 (±433) days from the plasma sample. Aβ-PET data was acquired at LBNL on a Siemens ECAT EXACT HR PET scanner (n=32) or a Siemens Biograph PET-CT scanner (n=104), or at UCSF China Basin on a GE Discovery STE/VCT PET-CT scanner (n=32). We created a Distribution Value Ratio (DVR) (for PIB, when patients underwent 90 min acquisition) or 50-70 min SUVR images (for Florbetapir or PIB when patients only underwent 20 min PET acquisition) as previously described,[3,75] using tracer-specific reference regions: cerebellar grey matter for PIB and whole cerebellum for Florbetapir. Aβ-PET positivity was based on visual read as previously validated against neuropathological standards.[39,40]

Voxelwise analyses and result rendering

Voxelwise analyses were run in SPM12 to test the association between plasma markers and gray matter volume or FTP SUVR in the primary cohort (UCSF+ARTFL). Separate models were used for each pair of variable (pTau181-volume, NfL-volume, pTau181-FTP, NfL-FTP) and models were run on i) all participants with available data, ii) patients with a clinical diagnosis of MCI or AD only, iii) patients with a clinical diagnosis of FTLD only. Specific sample size for each analysis is indicated in the result section. Age was entered as a covariate in all models and total intracranial volume was entered in MRI models to control for inter-individual variability in head size. Resulting T-maps were thresholded (based on uncorrected $p<0.001$ at the voxel level with family wise error-corrected $p<0.05$ at the cluster level) and converted to R-maps using the CAT12 toolbox (www.neuro.uni-jena.de/cat/). Maps were rendered on a 3D brain surface using BrainNet Viewer[76] (www.nitrc.org/projects/bnv/) and default interpolation and perceptually uniform color scales (magma for MRI, viridis for tau-PET; https://matplotlib.org/).

An overview of the methods can be found in the Life Sciences Reporting Summary, published alongside this publication.

Data availability statement

All requests for raw and analyzed data and materials will be promptly reviewed by the corresponding author and the University of California San Francisco to verify if the request is subject to any intellectual property or confidentiality obligations. Some participant data not included in the paper were generated as part of clinical trials and may be subject to patient confidentiality limitations. Data and materials from FTLD participants enrolled in ARTFL are accessible via forms that can be found on the ARTFL website: https://www.rarediseasesnetwork.org/cms/artfl/Healthcare-Professionals/Collaborating. Other data and materials that can be shared will be released via a Material Transfer Agreement.

Code availability statement

All requests for code used for data analyses and data visualization will be promptly reviewed by the corresponding author and the University of California San Francisco to verify if the request is subject to any intellectual property, confidentiality or other licensing obligations. If there are no limitations, the corresponding author will communicate with the requester to share the code.

Extended Data

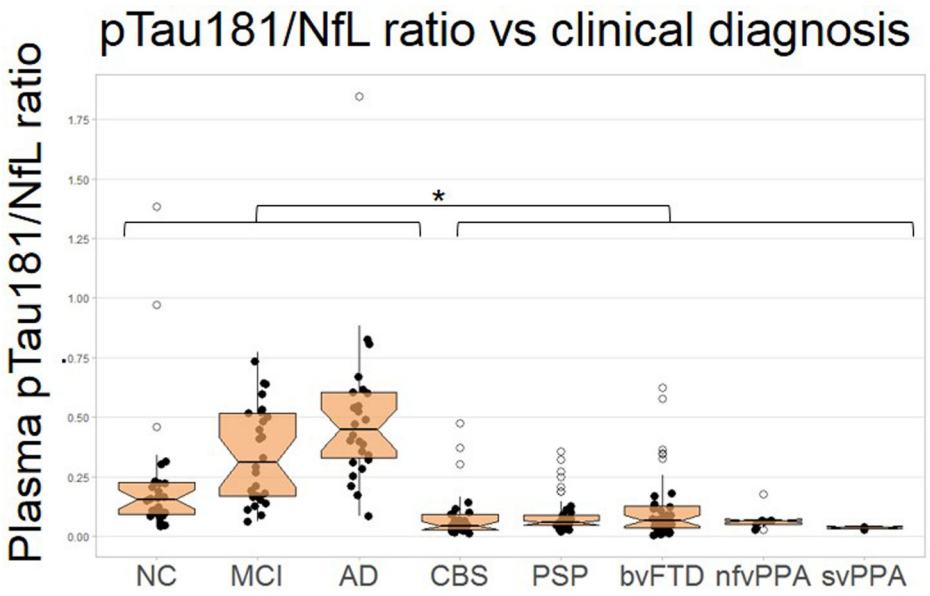

Extended Data Fig. 1. Plasma pTau/NfL ratio per clinical diagnosis

The ratio of pTau181/NfL was decreased in all FTLD diagnoses compared to controls, AD_{clin} and MCI patients (n=212). $^{**}p<0.001$ $^{*}p<0.05$

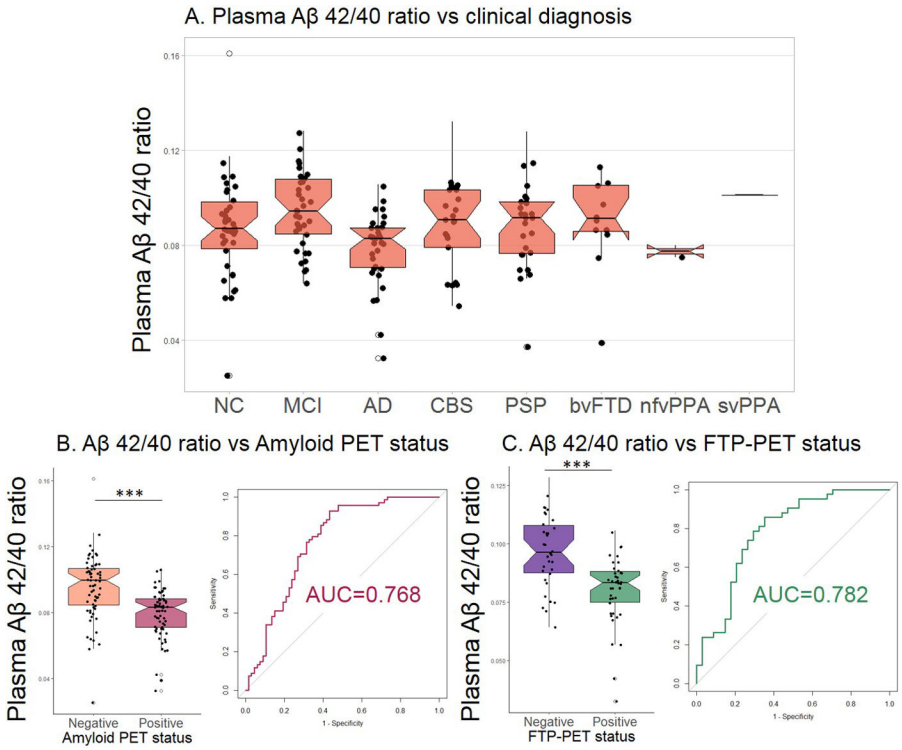

Extended Data Fig. 2. Plasma Aβ 42/40 ratio per clinical diagnosis and Amyloid PET and FTP-PET status

A. There was no difference in plasma Aβ 42/40 ratio between the different phenotypes(n=178). **B**. The Aβ 42/40 ratio was decreased in Amyloid PET positive cases (n=135). **C**. The Aβ 42/40 ratio was decreased in FTP-PET positive cases (n=76)

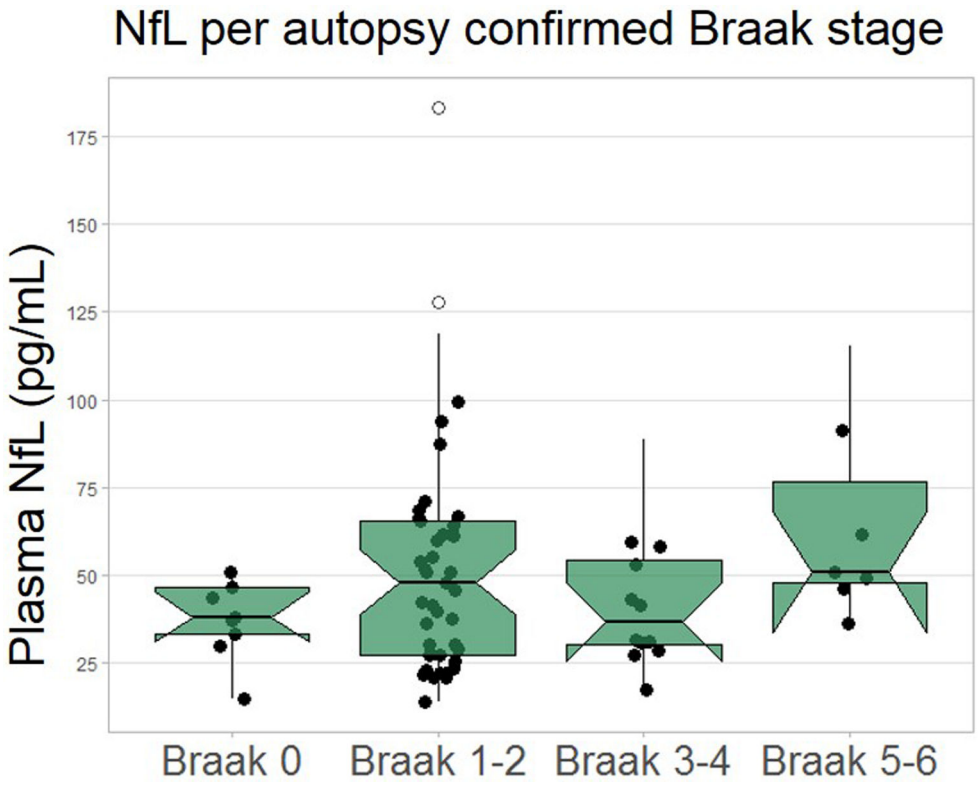

Extended Data Fig. 3. Plasma NfL concentrations per autopsy determined Braak stage
There was no difference in plasma NfL concentrations between the different Braak stages (n=69).

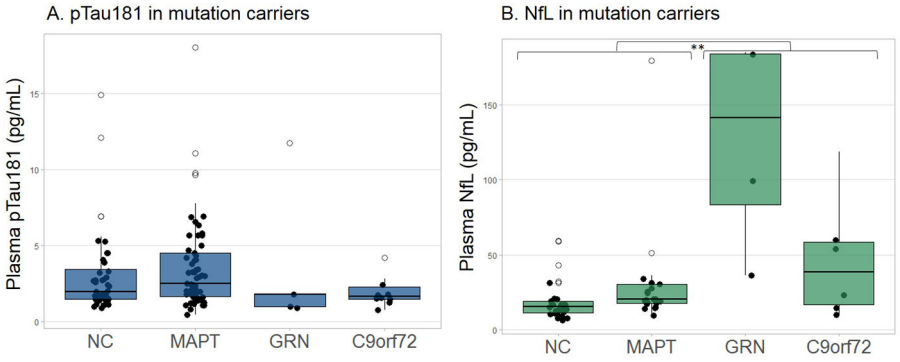

Extended Data Fig. 4. Plasma pTau181 and plasma NfL concentrations in mutation carriers

A. Plasma pTau181 concentrations did not differ between mutation carriers (n=120). **B**. Plasma NfL concentrations were elevated in *GRN* and *C9orf72* mutation carriers compared to the control group (p<0.0001) and MAPT mutation carriers (p<0.01) (n=59). **p<0.01

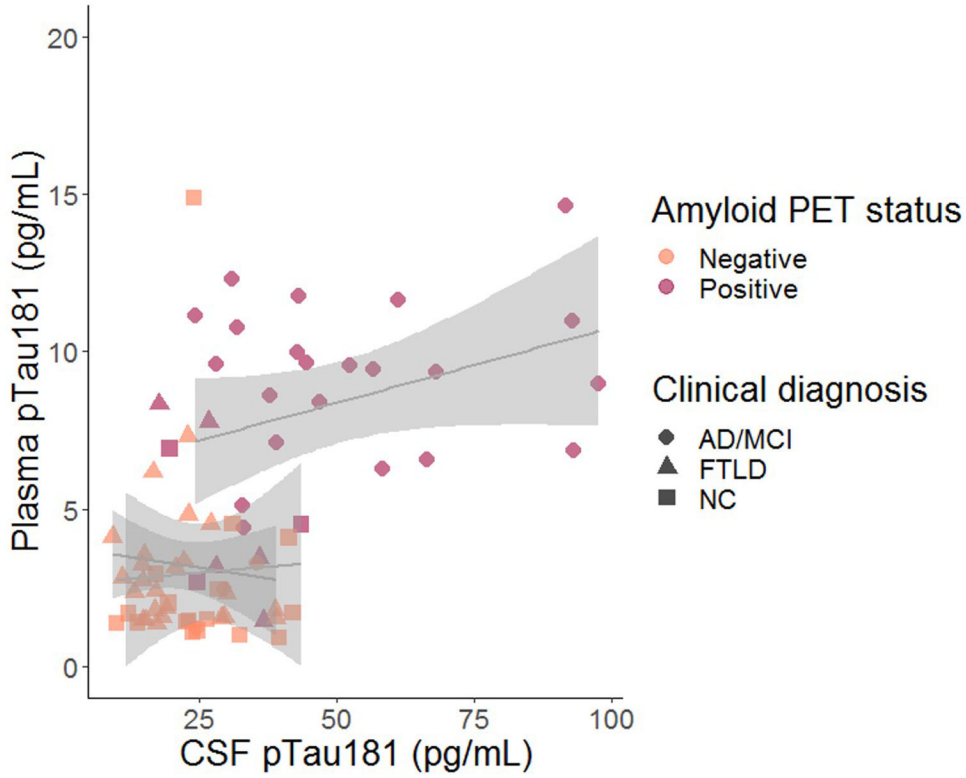

Extended Data Fig. 5. Association between plasma pTau181 and CSF pTau181

CSF pTau181 is associated with plasma pTau181 (β=0.51, p<0.0001; n=74), and is also associated within the AD/MCI (β=0.41, p=0.042; n=25), and the FTLD group (β=0.49, p<0.0001; n=29), but not in controls.

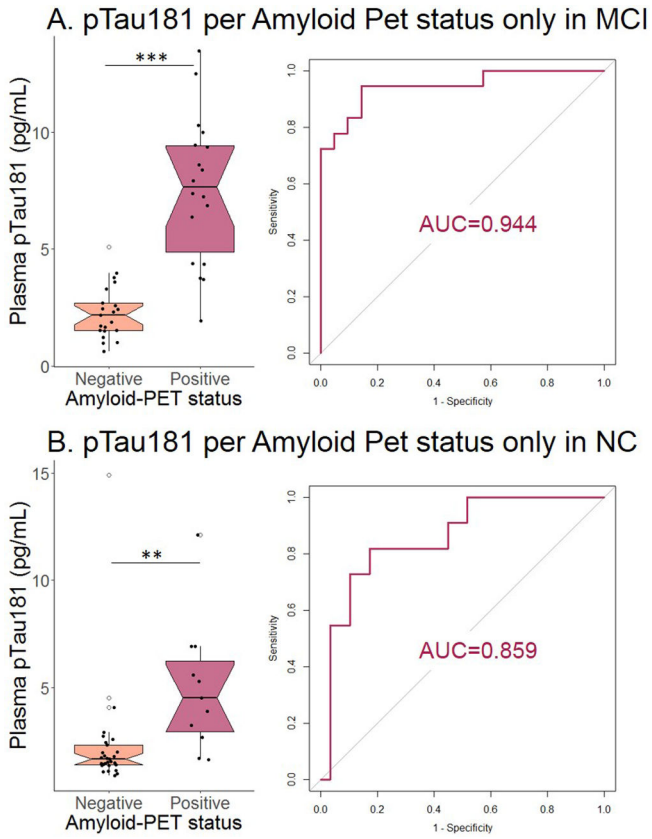

Extended Data Fig. 6. Receiver Operating Characteristic analyses of plasma pTau181 for Aβ-PET status in MCI patients and in controls

A. Plasma pTau181 concentrations are increased in Aβ-PET positive MCI cases. pTau181 could differentiate between Aβ-PET positive and negative cases (visual read). AUC=0.944 (95% CI: 0.873-1.000, $p<0.0001$, n= 18 Aβ-PET positive, 21 negative), with a cut-off of 8.4 pg/mL (0.944 sensitivity and 0.857 specificity). **B**. Plasma pTau181 concentrations are increased in Aβ-PET positive NC cases. pTau181 could differentiate between Aβ-PET positive and negative cases (visual read). AUC=0.859 (95% CI: 0.732-0.986, $p=0.001$, n=11 Aβ-PET positive, 29 negative), with a cut-off of 7.1 pg/mL (0.818 sensitivity and 0.828 specificity). Notch displays the confidence interval around the median. ***$p<0.0001$ **$p<0.01$

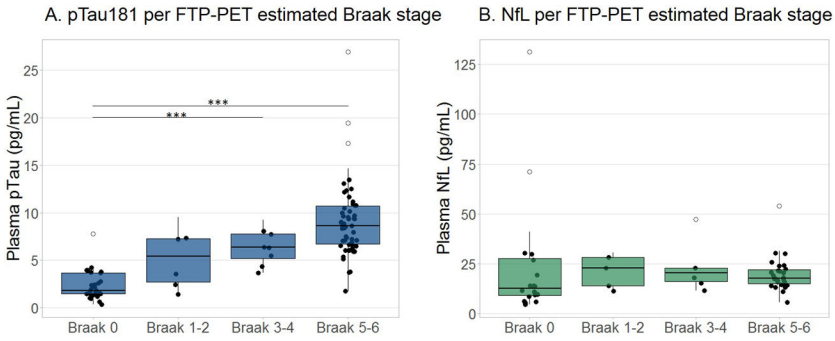

Extended Data Fig. 7. Plasma pTau181 and plasma NfL concentrations per FTP-PET estimated Braak stage

A. Plasma pTau181 was increased in Braak stage 5-6, and Braak stage 3-4 compared to Braak stage 0 (n=97). **B**. There was no difference in plasma NfL concentrations between the different Braak stages (n=61). ***p<0.0001

Supplementary Material

Refer to Web version on PubMed Central for supplementary material.

Acknowledgements:

The Advancing Research and Treatment for Frontotemporal Lobar Degeneration (ARTFL) investigators: L. Forsberg (Mayo R), D. Knopman (Mayo R), N. Graff-Radford (Mayo Jacksonville), M. Grossman (University of Pennsylvania), T. Huey (Columbia University), C. Onyike (Johns Hopkins University), D. Kaufer (University of North Carolina), E. Roberson (UAB), N. Ghoshal (Washington University), S. Weintraub (Northwestern), B. Appleby (Case Western), I. Litvan (UCSD), D. Kerwin (UTSW), M. Mendez (UCLA), Y. Bordelon (UCLA), C. Tartaglia (University of Toronto/Western Health Network), R. Hsiung (UBC), K. Domoto-Reilly (University of Washington), T. Foroud (NCRAD/Indiana University). S. Lowe designed and conducted Eli Lilly's study (NCT02624778) as well as provided a critical review of the manuscript. Data collection and dissemination of the data presented in this manuscript was supported by the LEFFTDS & ARTFL Consortium (LEFFTDS: U01 AG045390 [B. Boeve and H. Rosen]), funded by the National Institute on Aging and the National Institute of Neurological Diseases and Stroke; (ARTFL: U54 NS092089 [A. Boxer]), through the National Institute of Neurological Diseases and Stroke and the National Center for Advancing Translational Sciences, the Larry L. Hillblom Network and grant AG019724-17 [B. Miller]. Samples from the National Centralized Repository for Alzheimer's disease and Related Dementias (NCRAD), which receives government support under a cooperative agreement grant (U24 AG21886 [T. Foroud]) were used in this study. Imaging analyses were funded by Tau Consortium, National Institute on Aging grants (R01-AG045611 [G. Rabinovici], P50-AG023501 [B. Miller], P50-AG016574 [B. Boeve], P01-AG19724 [B. Miller], R01-AG038791 [A. Boxer], U54-NS092089 [A. Boxer], State of California Department of Health Services Alzheimer's Disease Research Centre of California grant (04-33516 [B. Miller]); Michael J Fox foundation (G. Rabinovici). Alzheimer's Association (AARF-16-443577, R. La Joie); K08AG052648 [S. Spina]. L. Grinberg receives support from K24AG053435. J. Rojas receives support from K23AG059888. Avid Radiopharmaceuticals enabled use of the [18F]AV1451 tracer by providing precursor, but did not provide direct funding and was not involved in data analysis or interpretation.

Role of funder/sponsor:

The funding agencies had no role in the design and conduct of the study, collection, management, analysis or interpretation of the data, preparation, review or approval of the manuscript or decision to submit the manuscript for publication.

References

1. Swine flu snipers, Alzheimer's drug push and Google's latest gaming bot. Nature 574 602–603 (2019). doi:doi: 10.1038/d41586-019-03266-0

2. Rabinovici GD et al. Association of Amyloid Positron Emission Tomography With Subsequent Change in Clinical Management Among Medicare Beneficiaries With Mild Cognitive Impairment or Dementia. JAMA - J. Am. Med. Assoc 94158, 1286–1294 (2019).
3. Landau SM et al. Comparing positron emission tomography imaging and cerebrospinal fluid measurements of beta-amyloid. Ann. Neurol 74, 826–836 (2013). [PubMed: 23536396]
4. Palmqvist S et al. Detailed comparison of amyloid PET and CSF biomarkers for identifying early Alzheimer disease. Neurology 85, 1240–1249 (2015). [PubMed: 26354982]
5. Rabinovici GD & Miller BL Frontotemporal Lobar Degeneration: Epidemiology, Pathophysiology, Diagnosis and Management. CNS Drugs 24, 375–398 (2010). [PubMed: 20369906]
6. Bahia VS, Takada LT & Deramecourt V Neuropathology of frontotemporal lobar degeneration: A review. Dement. Neuropsychol 7, 19–26 (2013). [PubMed: 29213815]
7. Buerger K et al. CSF phosphorylated tau protein correlates with neocortical neurofibrillary pathology in Alzheimer's disease. Brain 129, 3035–3041 (2006). [PubMed: 17012293]
8. Tapiola T et al. Cerebrospinal Fluid β-Amyloid 42 and Tau Proteins as Biomarkers of Alzheimer-Type Pathologic Changes in the Brain. Arch. Neurol 66, 382–389 (2009). [PubMed: 19273758]
9. Schöll M et al. Biomarkers for tau pathology. Mol. Cell. Neurosci (2018). doi:10.1016/j.mcn.2018.12.001
10. Marquié M et al. Validating novel tau positron emission tomography tracer [F-18]-AV-1451 (T807) on postmortem brain tissue. Ann. Neurol 78, 787–800 (2015). [PubMed: 26344059]
11. Ossenkoppele R et al. Discriminative accuracy of [18 F]flortaucipir positron emission tomography for Alzheimer disease vs other neurodegenerative disorders. JAMA - J. Am. Med. Assoc 320, 1151–1162 (2018).
12. Bacioglu M et al. Neurofilament Light Chain in Blood and CSF as Marker of Disease Progression in Mouse Models and in Neurodegenerative Diseases. Neuron 91, 56–66 (2016). [PubMed: 27292537]
13. Meeter LH, Kaat LD, Rohrer JD & Van Swieten JC Imaging and fluid biomarkers in frontotemporal dementia. Nature Reviews Neurology 13, 406–419 (2017). [PubMed: 28621768]
14. Khalil M et al. Neurofilaments as biomarkers in neurological disorders. Nat. Rev. Neurol 14, 577–589 (2018). [PubMed: 30171200]
15. Meeter LHH et al. Clinical value of neurofilament and phospho-tau/tau ratio in the frontotemporal dementia spectrum. Neurology 90, e1231–e1239 (2018). [PubMed: 29514947]
16. Ljubenkov PA et al. Cerebrospinal fluid biomarkers predict frontotemporal dementia trajectory. Ann. Clin. Transl. Neurol 5, 1250–1263 (2018). [PubMed: 30349860]
17. Scherling CS et al. CSF neurofilament concentration reflects disease severity in frontotemporal degeneration. Ann. Neurol 75, 116–126 (2014). [PubMed: 24242746]
18. Rojas JC et al. CSF neurofilament light chain and phosphorylated tau 181 predict disease progression in PSP. Neurology 90, e273–e281 (2018). [PubMed: 29282336]
19. Rohrer JD et al. Serum neurofilament light chain protein is a measure of disease intensity in frontotemporal dementia. Neurology 87, 1329–1336 (2016). [PubMed: 27581216]
20. Steinacker P et al. Serum neurofilament light chain in behavioral variant frontotemporal dementia. Neurology 91, e1390–e1401 (2018). [PubMed: 30209235]
21. Bridel C et al. Diagnostic Value of Cerebrospinal Fluid Neurofilament Light Protein in Neurology: A Systematic Review and Meta-analysis. JAMA Neurol. 1–14 (2019). doi:10.1001/jamaneurol.2019.1534
22. Preische O et al. Serum neurofilament dynamics predicts neurodegeneration and clinical progression in presymptomatic Alzheimer's disease. Nature Medicine 25, 277–283 (2019).
23. Mattsson N, Cullen NC, Andreasson U, Zetterberg H & Blennow K Association between Longitudinal Plasma Neurofilament Light and Neurodegeneration in Patients with Alzheimer Disease. JAMA Neurol. 1–9 (2019). doi:10.1001/jamaneurol.2019.0765
24. Nakamura A et al. High performance plasma amyloid-β biomarkers for Alzheimer's disease. Nature 554, 249–254 (2018). [PubMed: 29420472]

25. Ovod V et al. Amyloid β concentrations and stable isotope labeling kinetics of human plasma specific to central nervous system amyloidosis. Alzheimer's Dement. 13, 841–849 (2017). [PubMed: 28734653]
26. Janelidze S et al. Plasma β-amyloid in Alzheimer's disease and vascular disease. Sci. Rep 6, 1–11 (2016). [PubMed: 28442746]
27. Mielke MM et al. Association of plasma total tau level with cognitive decline and risk of mild cognitive impairment or dementia in the Mayo Clinic study on aging. JAMA Neurol. 74, 1073–1080 (2017). [PubMed: 28692710]
28. Mattsson N et al. Plasma tau in Alzheimer disease. Neurology 87, 1827–1835 (2016). [PubMed: 27694257]
29. Chen Z et al. Learnings about the complexity of extracellular tau aid development of a blood-based screen for Alzheimer's disease. Alzheimer's Dement. 15, 487–496 (2018). [PubMed: 30419228]
30. Hampel H et al. Blood-based biomarkers for Alzheimer disease: mapping the road to the clinic. Nat. Rev. Neurol 14, 639–652 (2018). [PubMed: 30297701]
31. Mielke MM et al. Plasma phospho-tau181 increases with Alzheimer's disease clinical severity and is associated with tau- and amyloid-positron emission tomography. Alzheimer's Dement. 14, 989–997 (2018). [PubMed: 29626426]
32. Ghetti B et al. Invited review: Frontotemporal dementia caused by microtubule-associated protein tau gene (MAPT) mutations: A chameleon for neuropathology and neuroimaging. Neuropathol. Appl. Neurobiol 41, 24–46 (2015). [PubMed: 25556536]
33. Maass A et al. NeuroImage Comparison of multiple tau-PET measures as biomarkers in aging and Alzheimer ' s disease. Neuroimage 157, 448–463 (2017). [PubMed: 28587897]
34. Braak H & Braak E Neuropathological stageing of Alzheimer-related changes. Acta Neuropathol. 82, 239–259 (1991). [PubMed: 1759558]
35. Braak H, Thal DR, Ghebremedhin E & Del Tredici K Stages of the pathologic process in alzheimer disease: Age categories from 1 to 100 years. J. Neuropathol. Exp. Neurol 70, 960–969 (2011). [PubMed: 22002422]
36. Rabinovici GD et al. Distinct MRI Atrophy Patterns in Autopsy-Proven Alzheimer's Disease and Frontotemporal Lobar Degeneration. Am J Alzheimers Dis Other Demen 22, 474–488 (2007). [PubMed: 18166607]
37. Halabi C et al. Patterns of striatal degeneration in frontotemporal dementia. Alzheimer Dis. Assoc. Disord 27, 74–83 (2013). [PubMed: 22367382]
38. Doraiswamy PM et al. Florbetapir F 18 amyloid PET and 36-month cognitive decline:a prospective multicenter study. Mol. Psychiatry 19, 1044–1051 (2014). [PubMed: 24614494]
39. Clark CM et al. Cerebral PET with florbetapir compared with neuropathology at autopsy for detection of neuritic amyloid-β plaques : a prospective cohort study. Lancet Neurol. 11, 669–678 (2012). [PubMed: 22749065]
40. La Joie R et al. Multisite study of the relationships between antemortem [11 C]PIB-PET Centiloid values and postmortem measures of Alzheimer's disease neuropathology. Alzheimer's Dement. 15, 205–216 (2019). [PubMed: 30347188]
41. Rabinovici GD et al. Amyloid vs FDG-PET in the differential diagnosis of AD and FTLD. Neurology 77, (2011).
42. Knopman DS et al. Entorhinal cortex tau, amyloid-beta, cortical thickness and memory performance in non-demented subjects. Brain 142, 1148–1160 (2019). [PubMed: 30759182]
43. Van Harten AC et al. Tau and p-tau as CSF biomarkers in dementia: A meta-analysis. Clin. Chem. Lab. Med 49, 353–366 (2011). [PubMed: 21342021]
44. Rivero-Santana A et al. Cerebrospinal Fluid Biomarkers for the Differential Diagnosis between Alzheimer's Disease and Frontotemporal Lobar Degeneration: Systematic Review, HSROC Analysis, and Confounding Factors. J. Alzheimer's Dis 55, 625–644 (2017). [PubMed: 27716663]
45. Del Campo M et al. Novel CSF biomarkers to discriminate FTLD and its pathological subtypes. Ann. Clin. Transl. Neurol 5, 1163–1175 (2018). [PubMed: 30349851]
46. Jones DT et al. In vivo 18 F-AV-1451 tau PET signal in MAPT mutation carriers varies by expected tau isoforms. Neurology 90, e947–e954 (2018). [PubMed: 29440563]

47. Smith R et al. 18F-AV-1451 tau PET imaging correlates strongly with tau neuropathology in MAPT mutation carriers. Brain 139, 2372–2379 (2016). [PubMed: 27357347]
48. La Joie R et al. Associations between [18 F]AV1451 tau PET and CSF measures of tau pathology in a clinical sample. Neurology 90, e282–e290 (2018). [PubMed: 29282337]
49. Pontecorvo MJ et al. Relationships between flortaucipir PET tau binding and amyloid burden, clinical diagnosis, age and cognition. Brain 140, 748–763 (2017). [PubMed: 28077397]
50. Jack CR et al. Longitudinal tau PET in ageing and Alzheimer's disease. Brain 141, 1517–1528 (2018). [PubMed: 29538647]
51. Palmqvist S et al. Performance of Fully Automated Plasma Assays as Screening Tests for Alzheimer Disease–Related β-Amyloid Status. JAMA Neurol. 1–10 (2019). doi:10.1001/jamaneurol.2019.1632
52. Lee SE et al. Clinicopathological correlations in corticobasal degeneration. Ann. Neurol 70, 327–340 (2011). [PubMed: 21823158]
53. McKhann GM et al. The diagnosis of dementia due to Alzheimer's disease: recommendations from the National Institute on Aging-Alzheimer's Association workgroups on diagnostic guidelines for Alzheimer's disease. Alzheimers. Dement 7, 263–269 (2011). [PubMed: 21514250]
54. Albert MS et al. The diagnosis of mild cognitive impairment due to Alzheimer's disease: recommendations from the National Institute on Aging-Alzheimer's Association workgroups on diagnostic guidelines for Alzheimer's disease. Alzheimers. Dement 7, 270–279 (2011). [PubMed: 21514249]
55. Hoglinger GU et al. Clinical Diagnosis of Progressive Supranuclear Palsy: The Movement Disorder Society Criteria HHS Public Access Author manuscript. Mov Disord 32, 853–864 (2017). [PubMed: 28467028]
56. Rascovsky K et al. Sensitivity of revised diagnostic criteria for the behavioural variant of frontotemporal dementia. Brain 134, 2456–77 (2011). [PubMed: 21810890]
57. Gorno-Tempini ML et al. Classification of primary progressive aphasia and its variants. Neurology 76, 1006–14 (2011). [PubMed: 21325651]
58. Lynch CA et al. The clinical dementia rating sum of box score in mild dementia. Dement. Geriatr. Cogn. Disord 21, 40–43 (2006). [PubMed: 16254429]
59. Folstein MF, Folstein SE & McHugh PR 'Mini-mental state'. A practical method for grading the cognitive state of patients for the clinician. J. Psychiatr. Res 12, 189–198 (1975). [PubMed: 1202204]
60. Kramer JH et al. Distinctive neuropsychological patterns in frontotemporal dementia, semantic dementia, and Alzheimer disease. Cogn. Behav. Neurol 16, 211–218 (2003). [PubMed: 14665820]
61. Satz P, Uchiyama C & White T Color Trails Test. Professional Manual. Odessa Psychol. Assess. Resour (1996).
62. Heaton R, Miller S, Taylor M & Grant I Revised Comprehensive Norms for an Expanded Halstead-Reitan Battery: Demographically Adjusted Neuropsychological Norms for African American and Caucasian Adults. PAR (2004).
63. Kaplan E, Goodglass H, Weintraub S & Goodglass H Boston naming test. (Lea & Febiger, 1983).
64. Yesavage JA et al. Development and validation of a geriatric depression screening scale: a preliminary report. J. Psychiatr. Res 17, 37–49 (1982). [PubMed: 7183759]
65. Pfeffer RI, Kurosaki TT, Harrah CHJ, Chance JM & Filos S Measurement of functional activities in older adults in the community. J. Gerontol 37, 323–329 (1982). [PubMed: 7069156]
66. Schwab R & England A Projection technique for evaluating surgery in Parkinson's disease in Billingham FH, Donaldson MC *, eds.* Third symposium on parkinson's disease. Edinburgh: Churchill Livingstone, 152–157 (1969).
67. Hochberg Y Controlling the False Discovery Rate : A Practical and Powerful Approach to Multiple Testing Author (s): Yoav Benjamini and Yosef Hochberg Source : Journal of the Royal Statistical Society . Series B (Methodological), Vol . 57 , No . 1 (1995), Publi. **57**, 289–300 (1995).
68. Youden WJ. Index for rating diagnostic tests. Cancer 32–35 (1950). [PubMed: 15405679]
69. ADNI. ADNI2 Procedures manual. BIOFLUIDS Collect. Process. Shipm 94 doi:10.1002/ejoc.201200111

70. Ashburner J & Friston KJ Unified segmentation. Neuroimage 26, 839–851 (2005). [PubMed: 15955494]

71. Malone IB et al. Accurate automatic estimation of total intracranial volume: a nuisance variable with less nuisance. Neuroimage 104, 366–372 (2015). [PubMed: 25255942]

72. Ashburner J & Friston KJ NeuroImage Diffeomorphic registration using geodesic shooting and Gauss – Newton optimisation. Neuroimage 55, 954–967 (2011). [PubMed: 21216294]

73. Southekal S et al. Flortaucipir F 18 Quantitation Using Parametric Estimation of Reference Signal Intensity. J. Nucl. Med 59, 944–951 (2018). [PubMed: 29191858]

74. Devous MD et al. Test–Retest Reproducibility for the Tau PET Imaging Agent Flortaucipir F 18. J. Nucl. Med 59, 937–943 (2018). [PubMed: 29284675]

75. Villeneuve S et al. Existing Pittsburgh Compound-B positron emission tomography thresholds are too high: statistical and pathological evaluation. Brain 138, 2020–2033 (2015). [PubMed: 25953778]

76. Xia M, Wang J & He Y BrainNet Viewer: a network visualization tool for human brain connectomics. PLoS One 8, e68910 (2013). [PubMed: 23861951]

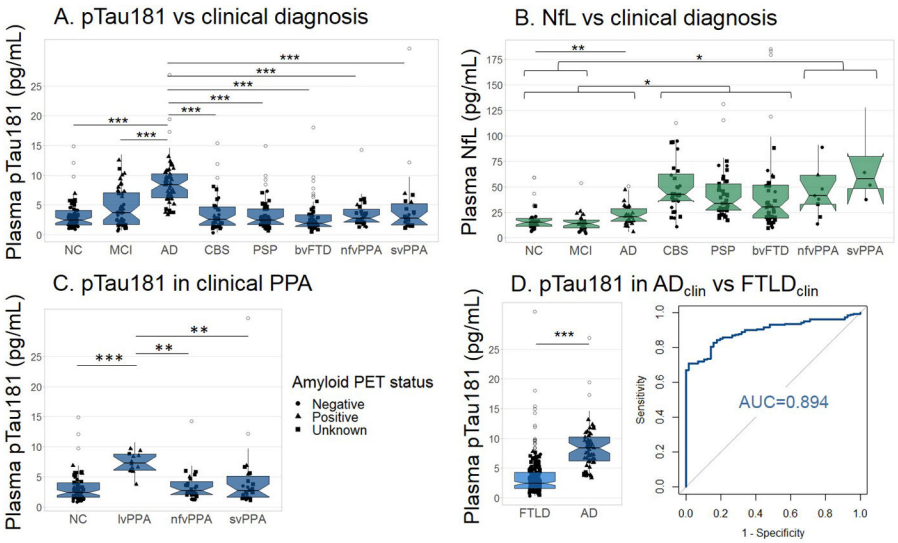

Figure 1. Plasma pTau181 and plasma NfL per clinical diagnosis.

A. pTau181 levels were elevated in AD_{clin} compared to non-AD clinical diagnoses (n=362). **B**. Plasma NfL were lower in controls, MCI and AD patients compared to CBS, PSP, and bvFTD, and NfL levels in NC and MCI were lower than in nfvPPA and svPPA patients (n=213). **C**. Plasma pTau181 levels are elevated in lvPPA, which is typically caused by AD, as compared to nfvPPA and svPPA, that are typically caused by FTLD, and controls (n=136). **D**. Plasma pTau181 concentrations were increased in AD_{clin} cases compared to FTLD clinical diagnoses and could differentiate between these groups (n=246). Notch displays the 95% confidence interval around the median. Shape reflects amyloid-PET status. ***p<0.0001, **p<0.01

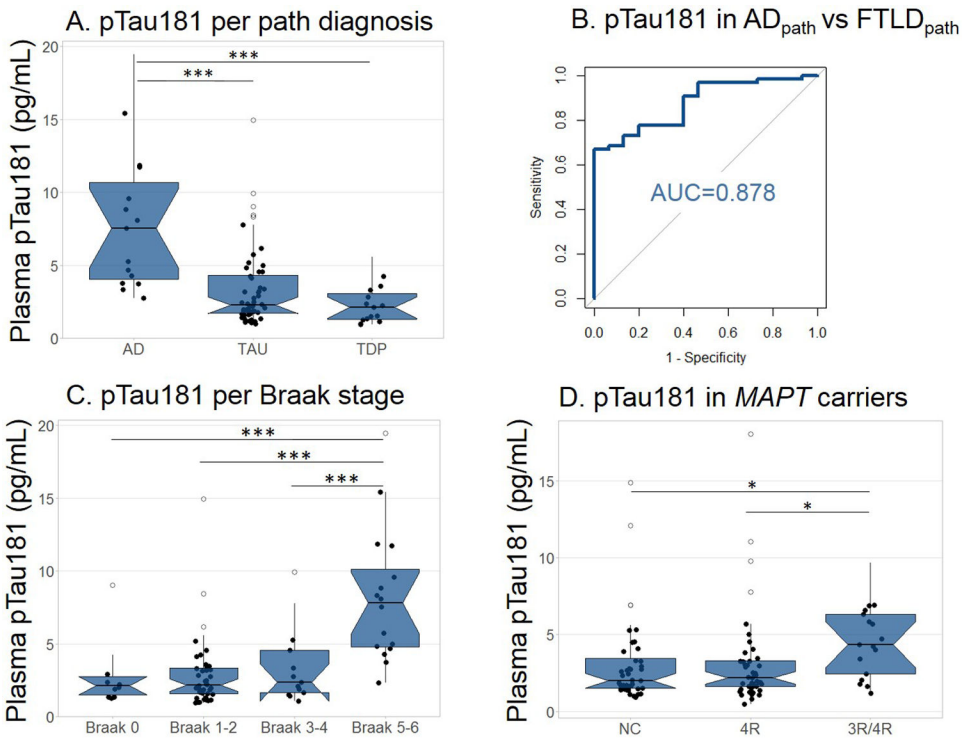

Figure 2. Plasma pTau181 in pathology-confirmed cases and *MAPT* mutation carriers

A. pTau181 levels are elevated in AD$_{path}$ (n=15, 7.5±8 pg/mL), compared to FTLD-tau (n=53, 3.4±3 pg/mL, p<0.0001), and FTLD-TDP (n=15, 2.1±2 pg/mL, *p*<0.0001). **B**. Plasma pTau181 levels differentiated between AD$_{path}$ and pathology-confirmed FTLD (FTLD-Tau and FTLD-TDP combined). **C.** Plasma pTau181 was increased in Braak stage 5-6 compared to Braak stage 0, stage 1-2, and stage 3-4 **D.** pTau181 concentrations were increased in *MAPT* mutation carriers with mixed 3R/4R tau pathology (n=17, 4.4±4 pg/mL), compared to those with 4R pathology (n=44, 2.2±2, *p*=0.024), and controls (n=44, 2.0±2, *p*=0.011). Biomarker concentrations shown as median ± IQR, ****p*<0.0001, **p*<0.05

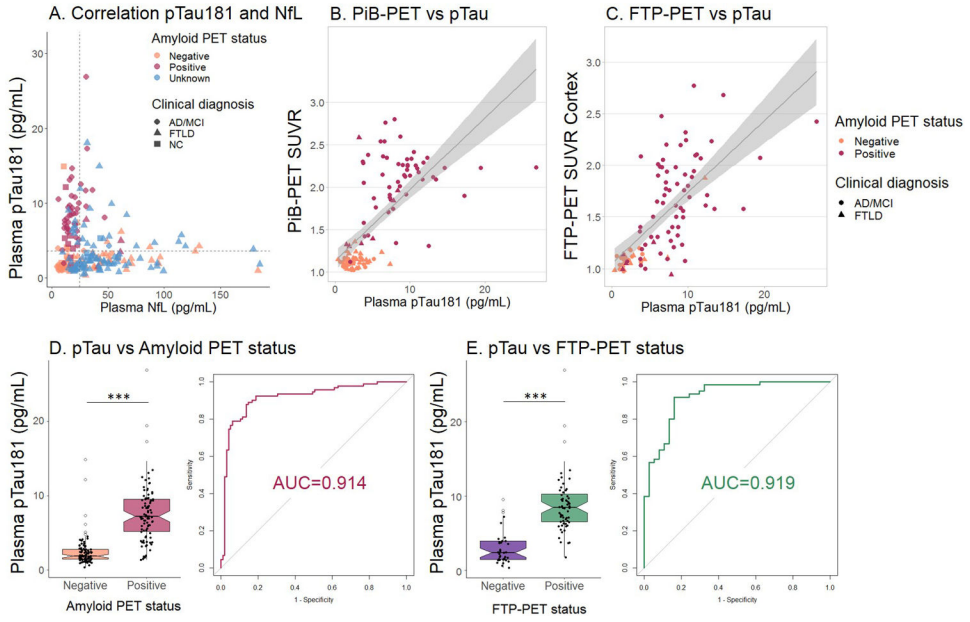

Figure 3. Association of pTau181 and NfL, PiB-PET SUVR, FTP-PET SUVR and Amyloid and FTP-PET status

A. Plasma pTau181 and plasma NfL measures are not correlated. Plasma pTau181 is increased in amyloid positive cases, and plasma NfL in FTLD cases. The dashed lines represent the uncorrected cut-off value for amyloid positivity (3.6 pg/mL) and the median concentration NfL (27.2 pg/mL) (n=213). The color coding shows Aβ-PET status and the shape coding shows diagnostic group. **B**. The association between plasma pTau181 and PiB-PET standardized uptake values (SUVRs), β=0.75, p<0.0001. Color coding per Aβ-PET status by visual read, shape coding per clinical diagnosis (n=124) **C**. The association between plasma pTau181 and FTP-PET SUVRs, β=0.73, p<0.0001. Color coding per Aβ-PET status by visual read, shape coding per clinical diagnosis (n=97). **D**. Plasma pTau181 concentrations are increased in Aβ-PET positive cases and can differentiate between Aβ-PET positive and negative cases (n=185, Aβ status determined based on visual read). **E**. Plasma pTau181 concentrations are increased in FTP-PET positive cases and can differentiate between FTP-PET positive and negative cases (based on binarized cortical SUVR values using a 1.22 threshold; n=97). Notch displays the confidence interval around the median. ***p<0.0001

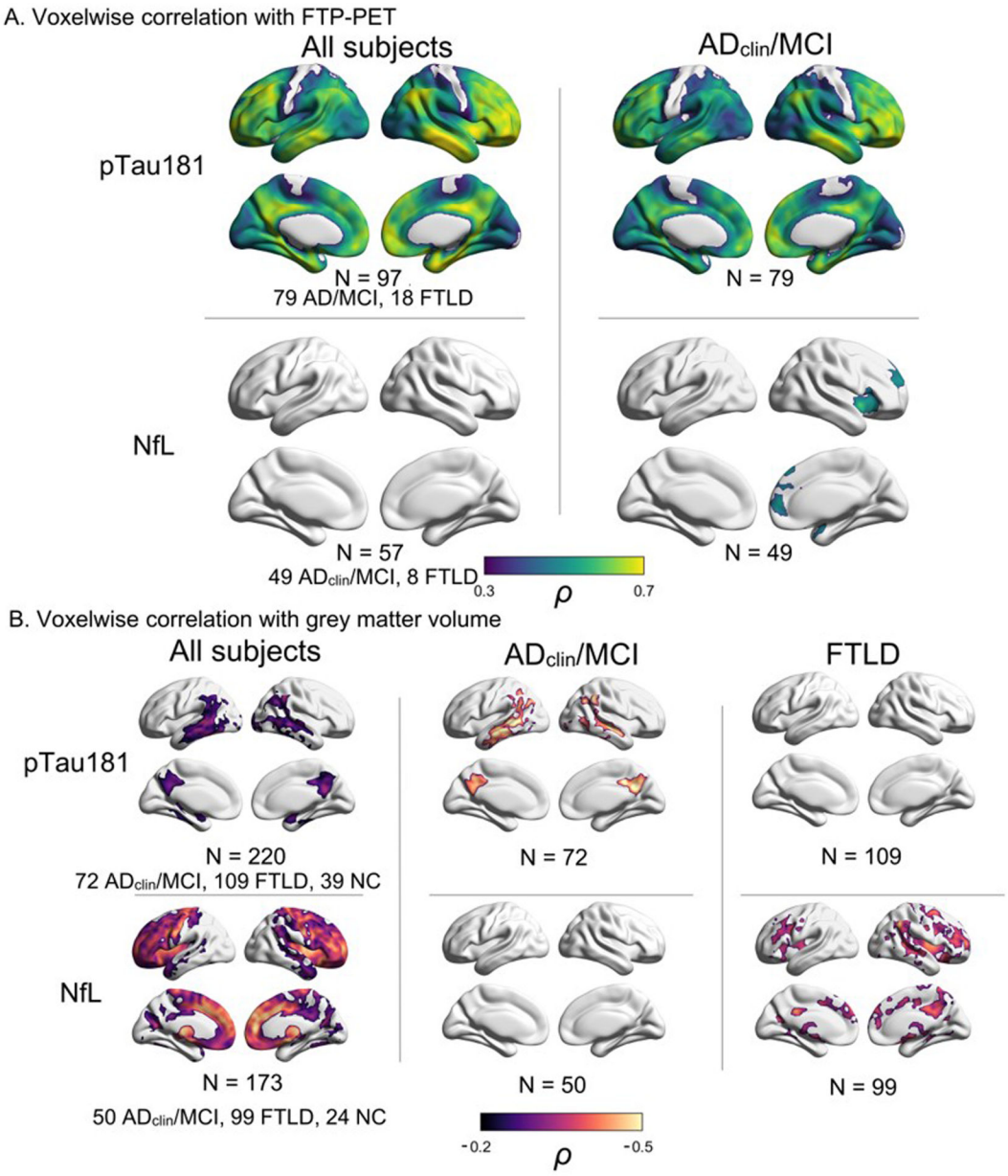

Figure 4. Voxelwise correlations of plasma pTau181 and plasma NfL with FTP-PET and grey matter atrophy

A. Regions of correlation between plasma pTau181 concentration and FTP-PET uptake were strongest in AD-specific brain regions: frontal and temporoparietal cortex, posterior cingulate and precuneus regions (ρ~0.75). There was no correlation of FTP-PET with plasma NfL in the whole cohort. In the AD_{clin}/MCI group correlations exist in the frontal and insular cortex (ρ~0.6). **B**. Negative correlations between plasma pTau181 and grey matter volume were highest in the bilateral temporal lobe and remained in the AD_{clin}/MCI group, but no correlation was found in the FTLD group. The correlation between plasma NfL and grey matter volume was highest in the right putamen and insular region (ρ~−0.5). The association remained in the FTLD group but was not found in the AD_{clin}/MCI group.

All correlations were thresholded based on an uncorrected $p<0.001$ at the voxel level and family wise error-corrected $p<0.05$ at the cluster level.

Table 1.

Participant characteristics, primary cohort

	NC (N=69)	MCI (N=47)	AD_{clin}* (N=56)	CBS (N=39)	PSP (N=48)	bvFTD (N=50)	nfvPPA (N=27)	svPPA (N=26)	All (N=362)
Sex, M/F	37/32	26/21	23/33	16/23	21/27	28/22	15/12	10/16	176/186
Age, y	60.6 (22)	60.8(14)	65.0 (9)	68.0 (8)	69.4 (7)	58.3 (9)	70.5 (7)[a,b]	69.3 (7)[a,b]	64.3 (13)
APOE E4 positivity N/total N (%)	18/65 (28%)	6/34 (18%)	20/29 (69%)	9/36 (25%)	9/47 (19%)	12/48 (25%)	5/20 (25%)	-	82/288 (28%)
Average disease duration	-	5.7 (3)	6.0 (3)	6.0 (4)	6.7 (3)	8.5 (8)	5.9 (2)	8.0 (4)	6.6 (5)
N	-	40	37	36	47	45	9	4	219
Disease severity									
CDR sum of boxes	0.0 (0)[b]	2.0 (1)[c]	4.8 (3)[a,b]	3.3 (3)[a]	4.7 (3)[a]	7.8 (3)[a,b]	3.4 (3)[a]	6.0 (3)[a,b]	3.6 (3)
N	65	47	56	39	46	31	27	26	337
SEADL, %	100 (2)	89 (18)	75 (16)	47 (22)[a,b]	43 (26)[a,b]	45 (19)[a,b]	67 (25)[a,b]	58 (19)[a,b]	62.8 (30)
N	34	14	6	29	45	21	22	17	188
FAQ	0.1 (0)[b,c]	4.6 (5)[a,c]	14.1 (8)[a,b]	11.9 (7)[a,b]	15.0 (6)[a,b]	20.5 (6)[a,b,c]	8.0 (8)[a,c]	16.0 (8)[a,b]	10.3 (9)
N	63	45	55	39	45	31	22	26	326
GDS	2.0 (2)[b,c]	6.3 (6)[a]	6.9 (5)[a]	10.6 (6)[a,b,c]	13.3 (6)[a,b,c]	6.8 (6)[a]	5.2 (6)	7.0 (4)	6.8 (6)
N	68	42	46	29	41	26	17	16	287
Neuropsychology									
MMSE	29.0 (1)[c]	26.8 (3)[c]	20.3 (6)[a,b]	23.4 (6)[a]	24.7 (4)[a,c]	20.7 (9)[a,b]	22.7 (6)[a]	19.2 (8)[a,b,c]	23.7 (6)
N	44	39	52	37	45	27	14	26	282
Modified trails test, seconds	26.6 (17)[c]	40.6 (21)[c]	89.7 (37)[a,b]	79.4 (40) [a,b]	90.4 (36) [a,b]	76.8 (40) [a,b]	91.3 (35) [a,b]	61.3 (9)	64.9 (40)
N	43	34	28	28	39	17	7	3	201
Stroop color naming, seconds	82.3 (16) [c]	71.0 (18) [c]	51.8 (22) [a,b]	44.3 (21) [a,b]	42.4 (20) [a,b]	52.0 (16) [a,b]	34.3 (16) [a,b]	30.5 (6) [a]	58.4 (24)
N	38	37	28	25	36	20	6	2	191
Semantic fluency, words per minute	16.2 (5) [c]	13.3 (4) [c]	9.5 (6) [a,b]	7.3 (4) [a,b]	6.6 (6) [a,b]	5.0 (3) [a,b]	3.7 (2) [a,b]	5.3 (2) [a]	9.8 (6)
N	41	37	36	32	46	22	6	3	225
BNT, number of words	14.7 (1) [c]	13.6 (2)	11.9 (3) [a]	12.8 (3)	13.1 (2)	10.9 (5) [a,b]	11.9 (4)	1.7 (2) [a,b,c]	12.8 (3)
N	43	36	36	31	46	24	7	3	228
D-word fluency, words per minute	10.7 (3) [c]	9.0 (3) [c]	5.2 (3) [a,b]	4.5 (3) [a,b]	5.2 (3) [a,b]	4.7 (4) [a,b]	4.8 (3) [a]	2.3 (1) [a]	6.9 (4)
N	38	38	34	18	3	22	6	3	187

	NC (N=69)	MCI (N=47)	AD_{clin} * (N=56)	CBS (N=39)	PSP (N=48)	bvFTD (N=50)	nfvPPA (N=27)	svPPA (N=26)	All (N=362)
Modified Rey copy, points	15.5 (1) *c*	15.2 (1) *c*	12.8 (4) *a,b*	10.9 (5) *a,b*	11.5 (3) *a,b*	15 (2)	13.2 (3)	15.8 (1)	13.5 (3)
N	37	39	36	27	39	21	5	4	210
Modified Rey recall, points	12.6 (2) *b,c*	8.7 (4) *a,c*	3.2 (4) *a,b*	7.4 (5) *a*	8.9 (3) *a*	8.6 (5) *a*	10.2 (5)	2.8 (4) *a*	8.2 (5)
N	37	39	37	27	38	23	5	4	212
Imaging									
Whole brain volume, L	1.1 (0.1)	1.1 (0.1)	1.0 (0.1)	1.0 (0.1) *a,b*	1.0 (0.1) *a*	0.9 (0.1) *a,b*	1.0 (0.2)	1.0 (0.1)	1.0 (0.1)
N	39	36	36	34	42	22	9	3	220
Bilateral hippocampal volume, mm^3	5332.8 (526) *c*	5119.7 (757)	4790.5 (704) *a*	5148.6 (660)	5188.9 (491)	4616.5 (612) *a*	5320.2 (871.2)	3958.9 (622) *a*	5063.3 (681)
N	39	35	36	34	42	22	9	3	220
FTP-PET SUVR cortex	-	1.2 (0) *c*	1.8 (0) *b*	1.1 (0) *c*	1.1 (0) *c*	1.1 (0) *c*	1.0 (0) *c*	1.4 (0)	1.5 (0)
N	-	31	48	4	4	5	2	3	97
PiB-PET SUVR	1.2 (0) *c*	1.5 (0) *c*	2.1 (0) *a,b*	1.3 (0) *c*	1.2 (0) *c*	1.2 (0) *c*	1.2 (0) *c*	1.1 (0) *c*	1.6 (1)
N	10	37	36	13	6	12	6	4	124
Amyloid-PET read, neg/pos	29/11	21/18	0/51	16/3	6/0	10/3	5/2	8/2	95/90
	40	39	51	19	6	13	7	10	185
Fluid biomarkers									
Plasma pTau181, pg/mL	2.4 (3) *c*	3.7 (6) *c*	8.4 (4) *a,b*	2.5 (3) *c*	2.4 (3) *c*	1.9 (2) *c*	2.7 (3) *c*	2.8 (4) *c*	4.3 (4)
N	69	47	56	39	48	50	27	26	362
Plasma NfL, pg/mL	15.2 (8) *c*	14.0 (8)	20.7 (14) *a*	42.6 (27) *a,b,c*	33.8 (26) *a,b,c*	30.3 (33) *a,b,c*	41.3 (29) *a,b*	58.0 (51) *a,b*	36.0 (30)
N	28	29	26	32	45	40	9	4	214
Plasma pTau181/NfL ratio	0.16 (0.1)	0.31 (0.4)	0.45 (0.3)	0.04 (0.1) *a,b,c*	0.06 (0.0) *a,b,c*	0.07 (0.1) *a,b,c*	0.07 (0.0) *b,c*	0.01 (0.0) *a,b,c*	0.24 (0.2)
N	28	28	26	32	45	40	9	4	213
CSF pTau181, pg/mL	24.4 (12) *b,c*	37.9 (24) *a*	45.8 (31) *a*	22.2 (11) *b,c*	18.1 (5)	20.7 (12) *b,c*	14.7 (15) *c*	27.0 (24)	32.8 (20)
N	20	9	16	11	4	9	3	2	74
Plasma Aβ 42 (pg/mL)	21.5 (6)	22.0 (8)	19.7 (7)	23.5 (9)	23.5 (8)	23.3 (6)	17.0 (2)	31.5 (−)	21.6 (8)
N	38	38	35	25	27	12	2	1	178
Plasma Abeta 40 (pg/mL)	248.4 (52)	236.6 (49)	245.9 (43)	262.8 (59)	252.6 (50)	231.3 (40)	218.9 (9)	311,5 (−)	249.4 (55)
N	38	38	35	25	27	12	2	1	178
Plasma Abeta 42/40 ratio	0.09 (0.0)	0.09 (0.0)	0.08 (0.0)	0.09 (0.0)	0.09 (0.0)	0.09 (0.0)	0.08 (0.0)	0.10 (−)	0.09 (0)
N	38	38	35	25	27	12	2	1	178

Values shown as mean (standard deviation), fluid biomarker values shown as median (IQR). Abbreviations: AD_{clin}, Clinical Alzheimer's disease; APOE, apolipoprotein E; BNT, Boston Naming Test; bvFTD, behavioral variant FTD; CDR, Clinical Dementia Rating; CBD, corticobasal degeneration; CSF, cerebrospinal fluid; FAQ, Functional Activities Questionnaire ; FTP-PET, 18F-Flortaucipir; GDS, Geriatric depression scale; MCI, mild cognitive impairment; MMSE, Mini-Mental State Test; Modified Rey copy, Modified Rey Benson Figure copy; NfL, neurofilament light chain; NC, Normal control; SEADL, Schwab and England Activities of Daily Living; SUVR, Standardized Uptake Value Ratio; PET, positron emission tomography; PiB, Pittsburgh Compound-B; pTau181, phosphorylated tau 181; PPA, primary progressive aphasia; PSP, progressive supranuclear palsy

Amyloid status was based on visual read of ^{18}F-AV-45 and PiB-PET imaging.

*AD_{clin} includes 14 logopenic variant PPA cases

a. Indicates a statistically significant difference between groups ($p < 0.05$) with NC in post hoc pairwise comparisons

b. $p < 0.05$ vs MCI

c. $p < 0.05$ vs AD

Table 2.

Diagnostic accuracy of plasma pTau181, NfL, Aβ42/40 ratio and CSF pTau181

Dx vs Dx	Test	n per group	AUC	95% CI	p-value*	Sensitivity	Specificity	Cut point (pg/mL)
FTP-PET positive vs negative, only MCI	pTau181, plasma	11 vs 20	0.977	0.929-1.000	<0.0001	0.909	0.950	8.1
Autopsy confirmed: AD vs FTLD-TDP	pTau181, plasma	15 vs 15	0.947	0.873-1.000	<0.0001	1.000	0.800	9.4
Aβ-PET positive vs negative, only MCI	pTau181, plasma	18 vs 21	0.944	0.873-1.000	<0.0001	0.944	0.857	8.4
Clinical AD vs FTLD	pTau181, CSF	16 vs 29	0.931	0.854-1.000	<0.0001	0.875	0.897	67.0
FTP-PET positive vs negative (all)	pTau181, plasma	60 vs 37	0.919	0.863-0.976	<0.0001	0.917	0,838	8.1
Aβ-PET positive vs negative (all)	pTau181, plasma	90 vs 95	0.914	0.869-0.958	<0.0001	0.889	0.853	8.0
Clinical AD vs FTLD	pTau181, plasma	56 vs 190	0.894	0.855-0.933	<0.0001	0.982	0.711	8.7
Autopsy confirmed: AD vs combined FTLD-TDP + FTLD-tau	pTau181, plasma	15 vs 67	0.878	0.798-0.957	<0.0001	1.000	0.672	9.5
Aβ-PET positive vs negative, healthy controls only	pTau181, plasma	11 vs 29	0.859	0.732-0.986	0.001	0.818	0.828	7.6
Autopsy confirmed: AD vs FTLD-tau	pTau181, plasma	15 vs 52	0.858	0.765-0.950	<0.0001	1.000	0.635	9.6
Autopsy confirmed: AD vs FTLD + mutation carriers	pTau181, plasma	15 vs 115	0.854	0.772-0.937	<0.0001	1.000	0.626	8.9
FTP-PET positive vs negative	Aβ42/40 ratio, plasma	42 vs 34	0.782	0.674-0.890	<0.0001	0.647	0.857	0.16
Aβ-PET positive vs negative	Aβ42/40 ratio, plasma	68 vs 67	0.768	0.686-0.849	<0.0001	0.567	0.926	0.15
Autopsy confirmed: AD vs FTLD-TDP	Plasma NfL	7 vs 14	0.765	0.557-0.973	0.052	0.643	1.000	53.7
Autopsy confirmed: FTLD-TDP vs FTLD-tau	pTau181, plasma	15 vs 52	0.664	0.499-0.829	0.054	0.981	0.333	9.6
Autopsy confirmed: AD vs combined FTLD-TDP + FTLD-tau	NfL, plasma	6 vs 63	0.656	0.369-0.774	0.209	0.429	1.000	48.7
Autopsy confirmed: FTLD-TDP vs FTLD-tau	NfL, plasma	13 vs 50	0.655	0.494-0.817	0.086	0.615	0.700	55.0
Autopsy confirmed: AD vs FTLD + mutation carriers	NfL, plasma	6 vs 70	0.633	0.439-0.828	0.281	0.414	1.000	48.0
FTP-PET positive vs negative	NfL, plasma	34 vs 27	0.606	0.446-0.765	0.159	0.824	0.556	64.5
Aβ-PET positive vs negative	NfL, plasma	51 vs 67	0.559	0.453-0.664	0.276	0.433	0.882	42.7

Cut-off value is adjusted for age, autopsy confirmed cut-off is adjusted for age and CDRsb.

Abbreviations: Aβ, beta-amyloid; AD, Alzheimer's disease; AUC, Area under the curve; CSF, Cerebrospinal fluid; FTP-PET, 18F-Flortaucipir PET; MCI, mild cognitive impairment; NfL, neurofilament light chain; PET, positron emission tomography; pTau181, phosphorylated tau 181

*p-value corrected for False Discovery Rate